

國立交通大學

電信工程學系

碩士論文

高車速下多輸入多輸出正交分頻多工系統中
結合資料偵測及通道估計之遞迴式接收機架構

An Iterative Receiver Architecture Based on Joint Data
Detection and Channel Estimation for High Mobility
MIMO OFDM Systems

研究生：李思潔

指導教授：黃家齊 博士

中華民國九十七年八月

高車速下多輸入多輸出正交分頻多工系統中
結合資料偵測及通道估計之遞迴式接收機架構

An Iterative Receiver Architecture Based on Joint Data Detection and
Channel Estimation for High Mobility MIMO OFDM Systems

研究生：李思潔

Student : Sih-Jie Li

指導教授：黃家齊 博士

Advisor : Dr. Chia-Chi Huang



A Thesis

Submitted to Department of Communication Engineering

College of Electrical and Computer Engineering

National Chiao Tung University

in partial Fulfillment of the Requirements

for the Degree of

Master of Science

in

Communication Engineering

August 2008

Hsinchu, Taiwan, Republic of China

中華民國九十七年八月

高車速下多輸入多輸出正交分頻多工系統中 結合資料偵測及通道估計之遞迴式接收機架構

學生：李思潔

指導教授：黃家齊博士

國立交通大學電信工程學系 碩士班

摘 要

對於應用於高移動通訊環境之正交分頻多工(Orthogonal Frequency Division Multiplexing, OFDM)系統，每一個 OFDM 符元期間的通道時變導致載波間干擾(Inter-carrier Interference, ICI)發生，使得系統效能降低。當載具速度、OFDM 符元期間增加，影響將更為嚴重。在這篇論文中，針對高移動性無線通道下之多輸入多輸出(MIMO) OFDM 系統，我們提出一個基於結合通道估計與資料偵測之遞迴式接收機架構，此架構主要由三級程序組成。在初始級，我們採用多重路徑干擾消除方法來粗略估計多重路徑延遲及多重路徑複數增益等通道參數；在追蹤級，我們先使用一個 β -追蹤器，之後再使用基於 V-BLAST 資料偵測之決策迴授離散傅立葉轉換通道估測方式，以估計每條路徑的增益平均值；在最後一級中，我們採用一個線性模型來近似每條路徑的時域變化，然後再利用一個二維的 V-BLAST 方法做資料決策，來達到消除 ICI 效應的目的。最後，我們以電腦模擬結果驗證了此遞迴式接收機在高移動性通道的效能增進。

An Iterative Receiver Architecture Based on Joint Data Detection and Channel Estimation for High Mobility MIMO OFDM Systems

Student : Sih-Jie Li

Advisors : Dr. Chia-Chi Huang

Department of Communication Engineering
National Chiao Tung University

ABSTRACT



For orthogonal frequency division multiplexing (OFDM) systems in high-mobility environment, channel variations within one OFDM symbol will introduce intercarrier interference (ICI), thus lowering the system performance. This becomes more severe as vehicle speed or OFDM symbol duration increase. In this paper, an iterative receiver architecture based on joint channel estimation and data detection is proposed for MIMO OFDM systems in mobile wireless channels. The iterative receiver mainly consists of three-stage processing. In the initialization stage, we employ a multipath interference cancellation technique to roughly estimate multipath delays and multipath complex gains through the preamble. In the tracking stage, a β -tracker is applied first, followed by decision-feedback (DF) DFT-based channel estimation which is based on V-BLAST data detection, so as to estimate the average channel variations of each path. In the final stage, we adopt a linear model to approximate time variations of each path, and a two-dimensional V-BLAST method is utilized to perform ICI cancellation and data detection. Finally, computer simulations are conducted to verify the performance of the iterative receiver in high-mobility channels.

誌 謝

感謝指導教授黃家齊老師對於我研究和學業上的指導與勉勵，給予我待人處事上的最佳模範。感謝老師在我研究所的兩年裡的指導與包容，使我在兩年的研究所生涯中獲益匪淺。感謝口試委員黃正光教授及陳紹基教授對本篇論文的指導與意見。

特別感謝博士班的古孟霖學長，在研究方面給予我莫大的幫助。在我研究上有困難時，不厭其煩地教導與關心，對我提出的任何疑問，都能耐心解說，使我得以順利完成論文。與學長的討論常使我收穫良多，學長的研究態度更是我的最好榜樣。

感謝冠群、小汪一直以來對我的照顧和生活上各方面的幫助，以及與人豪一起為實驗室電腦的維護。與你們的相處，輕鬆愉悅又不失溫馨，讓我度過這一段快樂時光。也感謝同屆同學阿威、文娟、建勳和學弟妹王森、曉顛以及實驗室所有成員的相互勉勵和關心。

最後，感謝我的家人，給予我精神上的鼓勵與支持，你們一直是支持我走下去的動力。

Contents

中文摘要	i
ABSTRACT	ii
誌謝	iii
Contents	iv
List of Figures	v
Chapter 1 Introduction	1
Chapter 2 MIMO OFDM System	5
2.1 Transmitted Signals	5
2.2 Channel Model	7
2.3 Received Signals	7
2.4 ICI on OFDM System	8
Chapter 3 V-BLAST Detection	11
Chapter 4 Iterative Receiver	16
4.1 Initialization Stage: The MPIC-Based Decorrelation Method	17
4.2 Tracking Stage: β -tracker	19
4.3 ICI Estimation	27
4.4 Two Dimensional V-BLAST Detection	33
Chapter 5 Performance Simulation	36
5.1 System Parameters	36
5.2 Simulation Results	37
Chapter 6 Conclusions	48
Bibliography	49

List of Figures

Fig. 1 MIMO OFDM system.....	5
Fig. 2 OFDM frame format	5
Fig. 3 Block diagram of the channel estimation in the tracking stage and the ICI cancellation in the final stage.....	16
Fig. 4 The MPIC-based decorrelation method in the initialization stage	19
Fig. 5 β -tracker followed by DF DFT-based channel estimation method in the tracking stage	26
Fig. 6 NMSE of the channel estimation with the assumption that the average channel variations $\mu_{l,0}^{(j,i)}$ for $l = 0, \dots, L^{(j,i)}$ are known versus E_b / N_o	32
Fig. 7 ICI effect from neighboring subcarriers with group size A	34
Fig. 8 BER performance in the two-path channel for normalized Doppler frequency $F_d * T = 0.02$	41
Fig. 9 BER performance in the ITU Veh-B channel for normalized Doppler frequency $F_d * T = 0.02$	42
Fig. 10 BER performance in the two-path channel for normalized Doppler frequency $F_d * T = 0.05$	43
Fig. 11 BER performance in the ITU Veh-B channel for normalized Doppler frequency $F_d * T = 0.05$	44
Fig. 12 BER versus normalized Doppler frequency $F_d * T$ in the two-path channel at $E_b / N_o = 25\text{dB}$	45
Fig. 13 BER performance in the two-path channel for normalized Doppler frequency $F_d * T = 0.05$ with different group size.....	46
Fig. 14 BER performance in the ITU Veh-B channel for normalized Doppler frequency $F_d * T = 0.05$ with different group size.....	47

Chapter 1 Introduction

Orthogonal frequency division multiplexing (OFDM) [1] has been widely applied in wireless communication systems in recent years due to its capability of high-rate transmission and low-complexity implementation over frequency-selective fading channels. The signals received through the multipath channel suffer from severe intersymbol interference (ISI) since the delay spread becomes much larger than the symbol duration. In OFDM system, the entire channel bandwidth is divided into many narrow subchannels, which are transmitted in parallel. Therefore, the symbol duration is increased and the intersymbol interference (ISI) caused by the multipath environments is eliminated or mitigated. On the other hand, communications over multiple-input multiple-output (MIMO) channels also have been the subject of intense research over the past several years because MIMO channels can support much greater data rate and higher reliability. Spatial multiplexing is one promising technique, which can significantly increase the channel capacity by the use of multiple antennas at both the transmitter and receiver. MIMO system can be combined with OFDM system to achieve high spectral efficiency, which makes it an attractive technique for high data rate wireless applications.

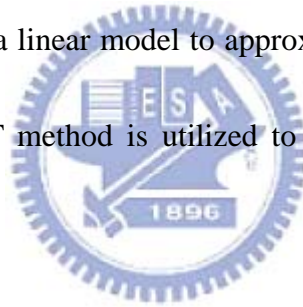
The received signals in MIMO OFDM system suffer from inter-antenna interference, hence, in this paper, we solve them by using V-BLAST data detection [2] with MMSE-SIC criterion. Moreover, in high mobility environment, the relative movement between transmitter

and receiver causes Doppler spread, and the channel variations due to high mobility give a time-selectivity in one OFDM symbol so that the multipath channel is no longer time invariant. Channel time-variations in one OFDM symbol may also arise the presence of an unknown carrier frequency offset, so the orthogonal property of OFDM system is destroyed and result in the effect of inter-carrier interference (ICI) among subcarriers which degrades the performance of OFDM systems [3] [4]. This becomes more severe as mobile speed, carrier frequency or OFDM symbol duration increases.

To reduce the ICI caused by channel variations, many approaches have been proposed. In [5], the authors proposed a self-cancellation scheme which sharpens the signal in frequency domain using the windowing operation in time domain to make subcarriers approximate nulls around the location of other subcarriers and, therefore, creates less ICI. In [6], it introduces a high performance equalization method by using MMSE with successive interference cancellation, but the computational complexity is very high.

[7] introduces two methods to mitigate ICI in an OFDM system with coherent channel estimation. Both methods use a piece-wise linear model to approximate channel time-variations. The first method extracts channel time-variations information from the cyclic prefix and the second method estimates these variations using both adjacent symbols. However, it acquires channel slopes by utilizing the redundancy of the cyclic prefix in the first method. While in the second method, the information of adjacent symbols has to be buffered.

In this paper, an iterative receiver architecture based on joint channel estimation and data detection is proposed to estimate the channel variations symbol by symbol, and a linear model is utilized to estimate the slope of each path without buffering information of adjacent symbols. The iterative receiver mainly consists of three-stage processing. In the initialization stage, we employ a multipath interference cancellation technique to roughly estimate multipath delays and multipath complex gains through the preamble. In the tracking stage, a β -tracker is applied, followed by decision-feedback (DF) DFT-based channel estimation along with V-BLAST data detection, so as to estimate the average channel variations of each path. In the final stage, we adopt a linear model to approximate time variations of each path, and a two-dimensional V-BLAST method is utilized to perform ICI cancellation and data detection.



The rest of this paper is organized as follows. In Chapter 2, we describe a MIMO OFDM system. The V-BLAST with MMSE-SIC detection algorithm is introduced briefly in Chapter 3. In Chapter 4, we present the MPIC-based decorrelation method in the initialization stage. Next, a β -tracker is developed in the tracking stage, and an ICI estimation is presented in the final stage. We then utilize the two dimensional V-BLAST detection to perform ICI cancellation and data detection. We present our computer simulation and performance evaluation results in Chapter 5. Finally, some conclusions are drawn in Chapter 6.

Notations: Boldface letters denote matrices, column vectors, and sets. The superscripts

$(\cdot)^*$ and $(\cdot)^H$ stand for complex conjugate and Hermitian respectively. The column vector \mathbf{x} can be explicitly expressed by $\langle x_1, \dots, x_{|\mathbf{x}|} \rangle$ or $\langle x_i : i \in \{1, \dots, |\mathbf{x}|\} \rangle$, where $|\mathbf{x}|$ is the dimension of the vector \mathbf{x} . The notation $\{\dots\}$ denotes a set, e.g. a set $\mathbf{x} = \{x_1, \dots, x_{|\mathbf{x}|}\}$, and the cardinality of the set \mathbf{x} is denoted by $|\mathbf{x}|$. Further, the set can be expressed in a compact form $\{x_i : i \in \{1, \dots, |\mathbf{x}|\}\}$.



Chapter 2 MIMO OFDM System

2.1 Transmitted Signals

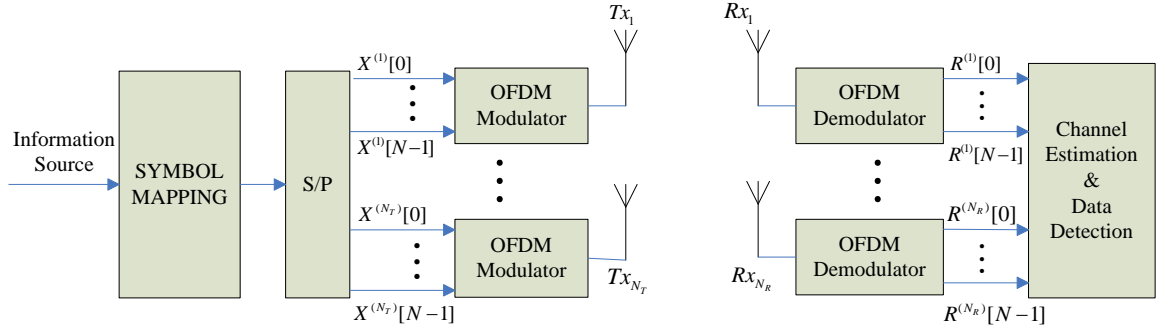


Fig. 1 MIMO OFDM system



Fig. 2 OFDM frame format

Fig. 1 and Fig. 2 illustrate a MIMO OFDM system and its frame format. We consider a MIMO OFDM system with N_T transmit and N_R receive antennas, employing N subcarriers among which M subcarriers are used to transmit data symbols plus pilot tones and the other $N - M$ subcarriers are used as either a DC subcarrier or virtual subcarriers at the two edges to avoid the aliasing problem at the receiver. Assume that the sets of data and pilot subcarriers indices are denoted as \mathbf{Q} and \mathbf{J} , respectively, where $\mathbf{Q}, \mathbf{J} \subseteq \mathbf{\Omega}$ and $\mathbf{\Omega} = \{0, \dots, N - 1\}$ is the set of the total subcarrier indices. The information source bits are first mapped into QPSK data symbols and are converted into N parallel data substreams through a serial to parallel (S/P) block. At the i th transmit antenna, $|\mathbf{Q}|$ QPSK data symbols $X^{(i)}[k]$,

for $k \in \mathbf{Q}$, and $|\mathbf{J}|$ pilot symbols $X^{(i)}[k]$, for $k \in \mathbf{J}$, are modulated onto M subcarriers via a N -point inverse Fast Fourier Transform (IFFT) unit to produce time domain samples after insertion of $N - M$ zeros for DC and virtual subcarriers.

$$\begin{aligned} x^{(i)}[n] &= \text{IFFT} \{ X^{(i)}[k] \} \\ &= \frac{1}{N} \sum_{k=0}^{N-1} X^{(i)}[k] e^{j2\pi kn/N}, \quad 0 \leq n \leq N-1. \end{aligned} \quad (2.1)$$

where $X^{(i)}[k]$ represents the transmitted data point at the k th subcarrier from the i th transmit antenna and $x_n^{(i)}$ is the time domain sequence. A cyclic prefix (CP) is then added in front of each OFDM data symbol to eliminate intersymbol interference (ISI) caused by multipath channels as follows:

$$\mathbf{x}_{cp}^{(i)} = \langle x^{(i)}[n] : N - G \leq n \leq N - 1 \rangle \quad (2.2)$$

where G is the length of guard interval. And we assume that the normalized length of the channel is always less than or equal to G in this paper to make sure that there is no ISI after removing the guard interval. As shown in Fig. 2, each OFDM frame starts with a CP-added preamble which occupies one OFDM symbol and is followed by D consecutive OFDM data symbols. Specifically, pilot tones are alternatively inserted into the available pilot subcarriers to avoid inter-antenna interference at the receiver side, and the pilot preamble in frequency domain is denoted by $P^{(i)}[k]$, for $k \in \mathbf{Q} \cup \mathbf{J}$ and $i = 1, \dots, N_T$.

2.2 Channel Model

In wireless communication, there may be more than one path from transmitter to receiver. Received signals come from multiple paths may be due to atmospheric reflection, refraction, or reflection from buildings and other objects. Such environment is called a multipath channel. The complex baseband representation of impulse response for a mobile wireless channel between the i th transmit antenna and the j th receive antenna can be described by

$$h^{(j,i)}[t, \tau] = \sum_{l=0}^{L^{(j,i)}-1} \mu_l^{(j,i)}(t) \delta[\tau - \tau_l^{(j,i)}] \quad (2.3)$$

where $\mu_l^{(j,i)}(t)$ is the complex Gaussian fading gain of the l th path, $\tau_l^{(j,i)}$ is the excess delay in samples of the l th path, $\delta[\tau]$ is a Kronecker delta function, and $L^{(j,i)}$ is the number of resolvable paths. All paths $\mu_l^{(j,i)}(t)$, for $0 \leq l \leq L^{(j,i)} - 1$, are assumed to be independent of each other and generated from Jakes' model. Thus, for OFDM systems with proper cyclic extension and sample timing, the channel frequency response can be expressed as

$$H^{(j,i)}[t, k] = \sum_{l=0}^{L^{(j,i)}-1} \mu_l^{(j,i)}(t) \exp\{-j2\pi k \tau_l^{(j,i)} / N\} \quad (2.4)$$

where k is the subcarrier index.

2.3 Received Signals

We assume that both timing and carrier frequency synchronization are perfect, and that the length of channel impulse response (CIR) is always shorter than the length of the CP so as to

remove CP correctly. Let T_s be the sampling period, then $T = T_s \times (N + G)$ is the time duration of one OFDM symbol after adding the guard interval. $h_l^{(j,i)}[n] = \mu_l^{(j,i)}(t = n \times T_s)$ represents the l th channel tap at time instant $t = n \times T_s$ corresponding to the i th transmit antenna and the j th receive antenna. A constant channel is assumed over the time interval $n \times T_s \leq t < (n+1) \times T_s$ with $t=0$ indicating the start of the data part of the symbol. $h_l^{(j,i)}[n]$ for $-G \leq n \leq -1$ and $0 \leq n \leq N-1$ represents the l th channel tap in the guard interval and data interval respectively.

Then the received signal $\mathbf{r}^{(j)}$ at the j th receive antenna is the superposition of all distorted transmitted signals, which can be expressed as follows:

$$r^{(j)}[n] = \sum_{i=1}^{N_T} \sum_{l=0}^{L^{(j,i)}-1} h_l^{(j,i)}[n] x^{(i)} \left[\left((n-l) \right)_N \right] + z^{(j)}[n], \quad 0 \leq n \leq N-1. \quad (2.5)$$

where $\left(() \right)_N$ represents a cyclic shift in the base of N and $z^{(j)}[n]$ represents a sample of uncorrelated additive white Gaussian noise (AWGN) with zero-mean and variance σ_z^2 on the j th receive antenna.

2.4 ICI on OFDM System

After the OFDM demodulator in Fig. 1, the received OFDM data symbols at the j th receive antenna in frequency domain are given by

$$R^{(j)}[k] = FFT \left\{ r^{(j)}[n] \right\} = \sum_{n=0}^{N-1} r^{(j)}[n] e^{-\frac{j2\pi nk}{N}} \quad 0 \leq k \leq N-1 \quad (2.6)$$

Substitute (2.1) (2.3) (2.5) into (2.6), we will find the relationship between $R^{(j)}[k]$ and

$X^{(i)}[k]$ which can be derived as follows:

$$\begin{aligned}
R^{(j)}[k] &= \sum_{n=0}^{N-1} \left(\sum_{i=1}^{N_r} \sum_{l=0}^{L^{(j,i)}-1} h_l^{(j,i)}[n] x^{(i)} \left[\left((n-l) \right)_N \right] + z^{(j)}[n] \right) e^{-\frac{j2\pi nk}{N}} \\
&= \sum_{i=1}^{N_r} \left(\sum_{n=0}^{N-1} \sum_{l=0}^{L^{(j,i)}-1} h_l^{(j,i)}[n] x^{(i)} \left[\left((n-l) \right)_N \right] e^{-\frac{j2\pi nk}{N}} \right) + \sum_{n=0}^{N-1} z^{(j)}[n] e^{-\frac{j2\pi nk}{N}} \\
&= \sum_{i=1}^{N_r} \left(\sum_{n=0}^{N-1} \sum_{l=0}^{L^{(j,i)}-1} h_l^{(j,i)}[n] \left(\frac{1}{N} \sum_{m=0}^{N-1} X^{(i)}[m] e^{-\frac{j2\pi ml}{N}} e^{\frac{j2\pi mn}{N}} \right) e^{-\frac{j2\pi nk}{N}} \right) + Z^{(j)}[k] \quad (2.7) \\
&= \sum_{i=1}^{N_r} \left(\sum_{m=0}^{N-1} \sum_{l=0}^{L^{(j,i)}-1} \left(\frac{1}{N} \sum_{n=0}^{N-1} h_l^{(j,i)}[n] e^{-\frac{j2\pi n(k-m)}{N}} \right) e^{-\frac{j2\pi ml}{N}} X^{(i)}[m] \right) + Z^{(j)}[k] \\
&= \sum_{i=1}^{N_r} \left(\sum_{m=0}^{N-1} \frac{1}{N} \sum_{l=0}^{L^{(j,i)}-1} F_l^{(j,i)}(k-m) e^{-\frac{j2\pi ml}{N}} X^{(i)}[m] \right) + Z^{(j)}[k]
\end{aligned}$$

$$\begin{aligned}
R^{(j)}[k] &= \sum_{i=1}^{N_r} \sum_{m=0}^{N-1} H^{(j,i)}[k, m] X^{(i)}[m] + Z^{(j)}[k] \\
&= \sum_{i=1}^{N_r} \left(H^{(j,i)}[k, k] X^{(i)}[k] + \underbrace{\sum_{m=0, m \neq k}^{N-1} H^{(j,i)}[k, m] X^{(i)}[m]}_{ICI} \right) + Z^{(j)}[k] \quad (2.8)
\end{aligned}$$

for $k \in \mathbf{Q} \cup \mathbf{J}$, where $Z^{(j)}[k]$ denotes the FFT of $z^{(j)}[n]$ and the second term on the right hand side of (2.8) represents ICI due to the Doppler spread caused by high mobility and cannot be neglected as the maximum Doppler frequency increases. Define $F_l^{(j,i)}(k)$ as the DFT of the l th channel tap with respect to time-variation:

$$F_l^{(j,i)}(k) = \sum_{n=0}^{N-1} h_l^{(j,i)}[n] e^{-\frac{j2\pi nk}{N}} \quad 0 \leq l \leq G \text{ \& } 0 \leq k \leq N-1 \quad (2.9)$$

Then $H^{(j,i)}[k, m]$ which denotes the channel frequency response from the m th subcarrier on the k th one can be defined as

$$H^{(j,i)}[k, m] = \sum_{l=0}^{L^{(j,i)}-1} \left[\frac{1}{N} \sum_{n=0}^{N-1} h_l^{(j,i)}[n] e^{-\frac{j2\pi n(k-m)}{N}} \right] e^{-\frac{j2\pi ml}{N}} = \frac{1}{N} \sum_{l=0}^{L^{(j,i)}-1} F_l^{(j,i)}(k-m) e^{-\frac{j2\pi ml}{N}} \quad (2.10)$$

Furthermore,

$$H^{(j,i)}[k,k] = \sum_{l=0}^{L^{(j,i)}-1} \mu_{l,0}^{(j,i)} e^{-\frac{j2\pi kl}{N}} \quad (2.11)$$

where $\mu_{l,0}^{(j,i)} = \frac{1}{N} \sum_{n=0}^{N-1} h_l^{(j,i)}[n]$ is the average of the l th channel tap over the time duration of $0 \leq t \leq N \times T_s$. Therefore, $H^{(j,i)}[k,k]$ represents the DFT of this average.

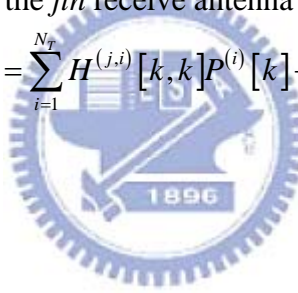
As the channel is time-invariant or we assume that the channel is quasi-static within one OFDM data symbol, $h_l[n]$ becomes a fixed complex fading gain (h_l). Then, because of the orthogonal property of the subcarriers, the second term of (2.8) becomes 0, which means no ICI, and (2.8) can be easily reduced as follows:

$$R^{(j)}[k] = \sum_{i=1}^{N_r} H^{(j,i)}[k,k] X^{(i)}[k] + Z^{(j)}[k] \quad (2.12)$$

And the received pilot preamble at the j th receive antenna can be described by

$$R_p^{(j)}[k] = \sum_{i=1}^{N_r} H^{(j,i)}[k,k] P^{(i)}[k] + Z^{(j)}[k] \quad (2.13)$$

for $k \in \mathbf{Q} \cup \mathbf{J}$.



Chapter 3 V-BLAST Detection

In this chapter, the conventional V-BLAST detection method with MMSE-SIC algorithm is introduced to perform data detection in MIMO OFDM system. We first consider a MIMO system with N_T transmit and N_R receive antennas, which can achieve high data rates by transmitting simultaneously different data on the different transmit antennas, and $N_T \leq N_R$. A single data stream is split into N_T substreams, each of which is transmitted using one of the N_T transmit antennas. The transmit diversity introduces spatial interference. The signals transmitted from various antennas propagate over independently scattered paths and interfere with each other upon reception at the receiver. After passing through the channel (assuming quasi-stationary), each receive antenna receives the signals radiated from all N_T transmit antennas. Let $\mathbf{X} = [X_1, X_2, \dots, X_{N_T}]^T$ denote the vector of transmit symbols, then the corresponding received signal vector can be written as

$$\mathbf{R} = \mathbf{H}\mathbf{X} + \mathbf{Z} \quad (3.1)$$

where \mathbf{R} is an N_R -component column vector of the received signals across the N_R receive antenna, \mathbf{H} is a $N_R \times N_T$ matrix with $H_{j,i}$ representing the channel frequency response between transmit antenna i and receive antenna j , and \mathbf{Z} is the AWGN noise vector with zero mean and variance σ^2 .

In the MMSE detection algorithm with successive interference cancellation (MMSE-SIC) [8], the expected value of the mean square error between transmitted signal \mathbf{X} and a linear

combination of the received vector $\mathbf{w}^H \mathbf{R}$ is minimized as follows

$$\min E \left\{ (\mathbf{X} - \mathbf{w}^H \mathbf{R})^2 \right\} \quad (3.2)$$

where \mathbf{w} is an $N_R \times N_T$ matrix of linear combination coefficients given by

$$\mathbf{w}^H = (\mathbf{H}^H \mathbf{H} + \sigma^2 \mathbf{I}_{N_T})^{-1} \mathbf{H}^H \quad (3.3)$$

\mathbf{I}_{N_T} is an $N_T \times N_T$ identity matrix. Using \mathbf{w}_i^H , the decision statistics for the symbol sent from antenna i is obtained as

$$Y_i = \mathbf{w}_i^H \mathbf{R} \quad (3.4)$$

where \mathbf{w}_i^H is the i th row of \mathbf{w}^H consisting of N_R components. The estimate of the symbol sent from antenna i , denoted by \hat{X}_i , is obtained by making a hard decision on Y_i

$$\hat{X}_i = Q(Y_i) \quad (3.5)$$

In an algorithm with interference suppression only, the detector calculates the hard decisions estimates by using (3.4) and (3.5) for all transmit antennas.

In a combined interference suppression and interference cancellation algorithm, the interference contribution from already-detected components of \mathbf{X} is subtracted from the received signal vector, resulting in a modified received vector in which fewer interferers are present. As mentioned in [2], when interference cancellation is used, the order in which the components of \mathbf{X} are detected becomes important to the overall performance of the system. Let the ordered set $S \equiv \{k_1, k_2, \dots, k_{N_T}\}$ be a permutation of the integers $1, 2, \dots, N_T$ specifying the order in which components of the transmitted symbol vector \mathbf{X} are extracted.

The optimal detection order is determined to maximize the minimum post-detection SNR of all data streams. A result is that simply choosing the best post-detection SNR at each stage in the detection process leads to the globally optimum ordering, S_{opt} .

The receiver starts from first iteration ($i = 1$) whose detection order is k_1 and computes its signal estimate by using (3.4) and (3.5). The received signal \mathbf{R} in this iteration is denoted by \mathbf{R}_1 . For calculation of the next iteration ($i = 2$), the interference contribution of the hard estimate \hat{X}_{k_1} is subtracted from the received signal \mathbf{R}_1 and this modified received signal denoted by \mathbf{R}_2 is used in computing the decision statistics for iteration 2 from (3.4) and its hard estimate in Eq. (3.5). This process continues for all other iterations.

After detection of iteration i whose detection order is k_i , the hard estimate \hat{X}_{k_i} is subtracted from the received signal \mathbf{R}_i to remove its interference contribution, resulting in modified received signal \mathbf{R}_{i+1} :

$$\mathbf{R}_{i+1} = \mathbf{R}_i - \hat{X}_{k_i} (\mathbf{H})_{k_i} \quad (3.6)$$

where $(\mathbf{H})_{k_i}$ denotes the k_i th column of \mathbf{H} . The operation $\hat{X}_{k_i} (\mathbf{H})_{k_i}$ in (3.6) replicates the interference contribution caused by \hat{X}_{k_i} in the received vector. \mathbf{R}_{i+1} is the received vector which is free from interference coming from $\hat{X}_{k_1}, \hat{X}_{k_2}, \dots, \hat{X}_{k_i}$. For estimation of the next stage, this signal \mathbf{R}_{i+1} is used in (3.4) instead of \mathbf{R} . Finally, a deflated version of the channel matrix is calculated, denoted by $\mathbf{H}_{\bar{k}_i}$, by zeroing column k_1, k_2, \dots, k_i of \mathbf{H} . The deflation is needed as the interference associated with the current symbol has been estimated

and cancelled.

The full V-BLAST with MMSE-SIC detection algorithm is described as a recursive procedure, including determination of the optimal ordering, as follows:

Initialization :

$$\begin{aligned}\mathbf{R}_1 &= \mathbf{R} \\ \mathbf{G}_1^H &= (\mathbf{H}^H \mathbf{H} + \sigma^2 \mathbf{I}_{N_T})^{-1} \mathbf{H}^H \\ k_1 &= \arg \min_j \|(\mathbf{G}_1)_j\|^2\end{aligned}$$

Recursion :

$$\begin{aligned}\mathbf{w}_{k_i} &= (\mathbf{G}_i)_{k_i} \\ Y_{k_i} &= \mathbf{w}_{k_i}^H \mathbf{R}_i \\ \hat{X}_i &= Q(Y_{k_i}) \\ \mathbf{R}_{i+1} &= \mathbf{R}_i - \hat{X}_i (\mathbf{H})_{k_i} \\ \mathbf{H} &= \mathbf{H}_{-k_i} \\ \mathbf{G}_i^H &= (\mathbf{H}^H \mathbf{H} + \sigma^2 \mathbf{I}_{N_T})^{-1} \mathbf{H}^H \\ k_{i+1} &= \arg \min_{j \in \{k_1, \dots, k_i\}} \|(\mathbf{G}_{i+1})_j\|^2 \\ i &= i + 1\end{aligned}$$

where $(\mathbf{G}_i)_j$ is the j th column of \mathbf{G}_i , and $\|v\|$ is the Euclidean norm of the vector v .

Since the post-detection SNR for the k_i th detected component of \mathbf{X} is $SNR_{k_i} = \frac{|X_{k_i}|^2}{\sigma^2 \|\mathbf{w}_{k_i}\|^2}$,

$k_1 = \arg \min_j \|(\mathbf{G}_1)_j\|^2$ corresponds to the strongest detected component of \mathbf{X} . Similarly, k_i corresponds to the strongest detected component among the remaining $(N_T - i + 1)$ components. Thus, it determines the elements of S_{opt} , the optimal ordering.

The V-BLAST architecture is essentially a single carrier signal processing algorithm. Therefore, to combine it with OFDM, the V-BLAST detection process has to be performed on

every subcarrier at the receiver to achieve high data rate transmission in frequency selective fading channels. As OFDM effectively divides the frequency selective channel into a number of flat fading subchannels, the MIMO OFDM system comprises a number of narrow band MIMO systems on different subcarriers. As the same detection algorithm is used on each subcarrier, MIMO OFDM system is basically a per-subcarrier MIMO structure, which performs V-BLAST detection on each subcarrier.



Chapter 4 Iterative Receiver

The iterative receiver based on joint channel estimation and data detection mainly consists of three-stage processing. In this section, we first present the MPIC-based decorrelation method for the initialization stage. In the following tracking stage, we adopt a β -tracker followed by DF-DFT based channel estimation method to estimate the frequency response of average channel variations of each path. With the estimated channel frequency response, the detection of transmitted signals can be performed by applying V-BLAST with MMSE-SIC algorithm described in chapter 3. In the final stage, we approximate channel variations of each path with a linear model. Then, a two-dimensional V-BLAST method is utilized to perform ICI cancellation and data detection. The block diagram of the channel estimation in the tracking stage and the ICI cancellation in the final stage is shown in Fig. 3.

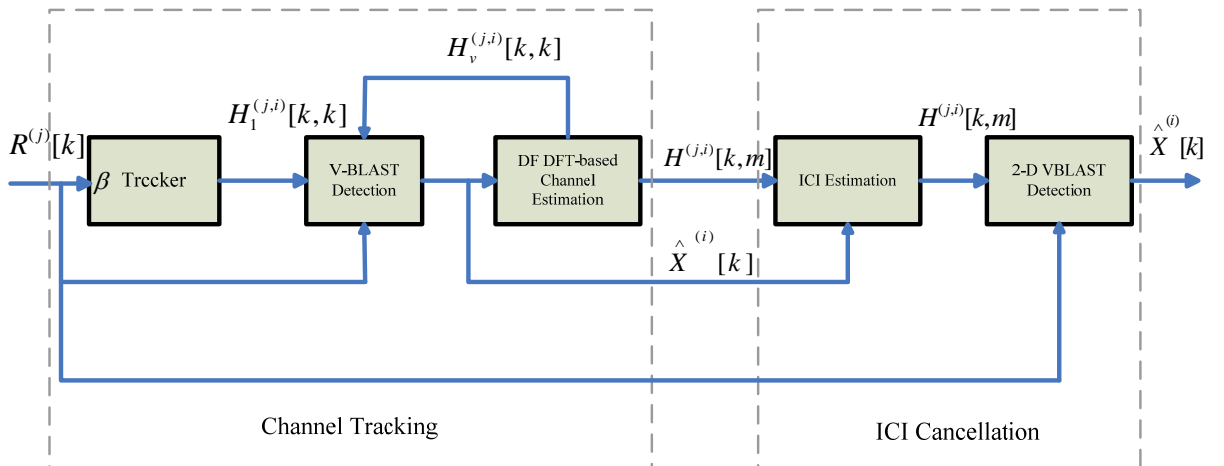


Fig. 3 Block diagram of the channel estimation in the tracking stage and the ICI cancellation in the final stage.

4.1 Initialization Stage: The MPIC-Based Decorrelation Method

In this stage, we roughly estimate multipath delays and multipath complex gains through the preamble placed at the beginning of each OFDM frame. We all know that CIR can be estimated by using the preamble placed at the beginning of each OFDM frame, while the difficulty is that for most wireless standards, the preamble does not have ideal auto-correlation due to the use of either guard band or non-equally spaced pilot tones. Fig. 4 outlines the MPIC-based decorrelation method to estimate CIR path-by-path by canceling out already known multipath interference. Since the preambles transmitted from different antennas do not interfere with each other at the receiver side, channel estimation can be independently performed for each transceiver antenna pair, and therefore the antenna indices j and i are omitted in the following. In step 1, we first define two parameters \mathbf{W}_b and N_p which represent a multipath observation window and a presumed number of paths in a mobile radio channel, respectively. Next, we calculate the cyclic cross-correlation $C_{RP}[\tau]$ between the received and the transmitted preamble by

$$C_{RP}[\tau] = IDFT \{ R_p[k] \cdot P^*[k] \}, \tau = 0, \dots, N-1 \quad (4.1)$$

The normalized cyclic auto-correlation $C_{PP}[\tau]$ of the transmitted preamble can also be calculated by

$$C_{PP}[\tau] = IDFT \{ P[k] \cdot P^*[k] \}, \tau = 0, \dots, N-1 \quad (4.2)$$

Both ρ and κ , which stand for a path counting variable and the number of legal paths

found by the MPIC-based decorrelation method, respectively, are initialized to zero. In step 2, we start by increasing the value of the path counting variable ρ by one, and picking only one path whose time delay $\tilde{\tau}_\rho$ yields the largest value in $|C_{RP}[\tau]|$, for $\tau \in \mathbf{W}_b$. If the time delay $\tilde{\tau}_\rho$ is larger than the length of the CP, this path is treated as an illegal path, and we discard it by setting $C_{RP}[\tilde{\tau}_\rho] = 0$. Otherwise, we increase the number of legal paths found, κ , by one, and then reserve this path as the κ th legal path with time delay $\hat{\tau}_\kappa = \tilde{\tau}_\rho$ and complex path gain $\hat{\mu}_\kappa = C_{RP}[\hat{\tau}_\kappa]$. The replica of the interference associated with this legal path is regenerated and subtracted from $C_{RP}[\tau]$ to obtain a refined cross-correlation function:

$$C_{RP}[\tau] \leftarrow C_{RP}[\tau] - \hat{\mu}_\kappa C_{PP}[\tau - \hat{\tau}_\kappa], \tau \in \mathbf{W}_b \setminus \{\tilde{\tau}_i : i = 1, \dots, \rho - 1\} \quad (4.3)$$

where “ \leftarrow ” is the assignment operation. We continue the iterative process of the step 2 until ρ reaches the presumed value of N_p .

```

Step1: Set preassumed number of paths  $N_p$  & observation window  $\mathbf{W}_b$ 
        Calculate  $C_{RP}[\tau]$  &  $C_{PP}[\tau]$  by
         $C_{RP}[\tau] = IDFT\{R_p[k] \cdot P^*[k]\}, \tau = 0, \dots, N-1$ 
         $C_{PP}[\tau] = IDFT\{P[k] \cdot P^*[k]\}, \tau = 0, \dots, N-1$ 
        Initialize  $\rho = 0$  and  $\kappa = 0$ 
Step2: Estimate multipath delays and complex gains coarsely:
        while  $\rho < N_p$ 
             $\rho \leftarrow \rho + 1$ 
             $\tilde{\tau}_\rho = \arg \max_{\tau \in \mathbf{W}_b} \{|C_{RP}[\tau]|\}$ 
            if  $\tilde{\tau}_\rho > G$ 
                 $C_{RP}[\tilde{\tau}_\rho] = 0$ 
            else
                 $\kappa \leftarrow \kappa + 1$ 
                find a legal path with time delay  $\hat{\tau}_\kappa = \tilde{\tau}_\rho$  & complex gain  $\hat{\mu}_\kappa = C_{RP}[\hat{\tau}_\kappa]$ 
                 $C_{RP}[\tau] \leftarrow C_{RP}[\tau] - \hat{\mu}_\kappa C_{PP}[\tau - \hat{\tau}_\kappa], \tau \in \mathbf{W}_b \setminus \{\tilde{\tau}_i : i = 1, \dots, \rho - 1\}$ 
            end
        end
    
```

Fig. 4 The MPIC-based decorrelation method in the initialization stage

4.2 Tracking Stage: β -tracker

Through the initialization stage, we are able to obtain information on the number of paths $\kappa^{(j,i)} (\leq N_p)$, the multipath delays $\hat{\tau}_l^{(j,i)}$, and the multipath complex gains $\hat{\mu}_l^{(j,i)}$, for $l \in \{1, \dots, \kappa^{(j,i)}\}$. Without loss of generality, we assume that the multipath delays do not vary over the duration of each OFDM frame. In this stage, we also suppose that the channel is quasi-static within one OFDM data symbol, which means the multipath complex gains of channel model are unchanged, so as to estimate the average channel variations of each path.

Accordingly, the corresponding channel estimator $\hat{H}^{(j,i)}[k,k]$ for the frequency response $H^{(j,i)}[k,k]$ can be formed by a summation of $\kappa^{(j,i)}$ exponential functions as follows:

$$\hat{H}^{(j,i)}[k,k] = \sum_{l=0}^{\kappa^{(j,i)}-1} \hat{\mu}_l^{(j,i)} \exp\left\{-j2\pi k \hat{\tau}_l^{(j,i)} / N\right\} \quad (4.4)$$

In this stage, a β -tracker followed by DF DFT-based channel estimation is applied to track channel. We start by utilizing the decision feedback (DF) DFT-based channel estimation method, using the ML criterion [9] [10][11][12], which is provided in the following:

$$\hat{\mathbf{H}}_v^{(j,i)} = \mathbf{F}_{DFT}^{(j,i)} \left(\mathbf{F}_{d,IDFT}^{(j,i)} \mathbf{F}_{d,DFT}^{(j,i)} \right)^{-1} \mathbf{F}_{d,IDFT}^{(j,i)} \left(\hat{\mathbf{X}}^{(i)} \right)^{-1} \tilde{\mathbf{R}}_v^{(j,i)} \quad (4.5)$$

where v is the iteration number from 1 to V , $\hat{\mathbf{H}}_v^{(j,i)} = \left\langle \hat{H}_v^{(j,i)}[k,k] : k \in \Omega = \{0, \dots, N-1\} \right\rangle$ is the estimated channel frequency response between the i th transmit antenna and the j th receive antenna at the v th iteration, $\hat{\mathbf{X}}^{(i)} = \text{diag} \left\{ \hat{X}^{(i)}[\Theta_1], \dots, \hat{X}^{(i)}[\Theta_{|\Theta|}] \right\}$ consists of the decision data symbols in which Θ is a subset of \mathbf{Q} used to track channel variations and $\hat{X}^{(i)}[k]$ can be obtained by applying the previously estimated channel frequency response to the V-BLAST data detection with respect to the received signals. $\mathbf{F}_{d,DFT}^{(j,i)}$ represents the $|\Theta| \times \kappa^{(j,i)}$ truncated DFT matrix whose (m,l) th entry is defined as $\exp\left\{-j2\pi \Theta_m \tau_l^{(j,i)} / N\right\}$, $\mathbf{F}_{d,IDFT}^{(j,i)}$ is the $\kappa^{(j,i)} \times |\Theta|$ truncated IDFT matrix which can be equivalently expressed as $\mathbf{F}_{d,IDFT}^{(j,i)} = \left(\mathbf{F}_{d,DFT}^{(j,i)} \right)^H$, and $\mathbf{F}_{DFT}^{(j,i)}$ is the $N \times \kappa^{(j,i)}$ truncated DFT matrix. For simplification, the subscripts ‘‘DFT’’ and ‘‘IDFT’’ are omitted, then $\mathbf{F}_{d,DFT}^{(j,i)}$, $\mathbf{F}_{d,IDFT}^{(j,i)}$ and $\mathbf{F}_{DFT}^{(j,i)}$ are replaced by $\mathbf{F}_d^{(j,i)}$, $\left(\mathbf{F}_d^{(j,i)} \right)^H$, and $\mathbf{F}^{(j,i)}$ respectively. We assume that the data interference signals from other transmit antennas can be reconstructed and cancelled perfectly from the received signals

$\mathbf{R}^{(j)}$. Thus, the refined signals corresponding to the (j, i) th antenna pair can be represented as

$$\tilde{\mathbf{R}}_v^{(j,i)} = \left\langle \tilde{R}_v^{(j,i)}[k] = R^{(j)}[k] - \sum_{m \neq i} \hat{H}^{(j,m)}[k, k] \hat{X}^{(m)}[k] = H^{(j,i)}[k, k] X^{(i)}[k] + Z[k], k \in \Theta \right\rangle \quad (4.6)$$

Moreover, since the refined signals from different antenna pair do not interfere with each other, we can perform the channel estimation for each transceiver antenna pair and, for simplification, the superscript “ (j, i) ” and “ (i) ” are dropped hereafter. Therefore, the DF-DFT based channel estimation method can be expressed as follows:

$$\hat{\mathbf{H}}_v = \mathbf{F} (\mathbf{F}_d^H \mathbf{F}_d)^{-1} \mathbf{F}_d^H \hat{\mathbf{X}}^{-1} \tilde{\mathbf{R}}_v \quad (4.7)$$

This is, however, not a good solution in fast time-varying channels because decision data symbols easily induce the error propagation effect. Therefore, pilot tones play an important role in fast fading channels. While in the slowly fading channels, decision data symbols are more reliable than pilot tones due to the number of data subcarriers are much more than pilot tones. Hence, we can modify the first iteration by adopting pilot tone as well as decision data symbols simultaneously to perform channel estimation at the first iteration. This, we modify the first iteration with $v=1$ by the β -tracker in which the current channel can be weighted with the channel estimated over data symbols in the previous time slot and the channel estimated over pilot signals in the current time slot due to that the current channel is related to the previous channel, which depends on how fast the channel varies. Therefore, The

β -tracker for the first iteration ($v=1$) can be described as follows:

$$\hat{\mathbf{H}}_v = (1 - \beta) \hat{\mathbf{H}}_{v-1} + \beta \hat{\mathbf{H}}_p \quad (4.8)$$

where $\hat{\mathbf{H}}_0$ represents the channel estimated over data symbols in previous time slot, $\hat{\mathbf{H}}_p = \mathbf{F}(\mathbf{F}_p^H \mathbf{F}_p)^{-1} \mathbf{F}_p^H \mathbf{X}_p^{-1} \mathbf{R}_p$ denotes the channel estimated by DF DFT-based channel estimation over pilot subcarriers in which \mathbf{X}_p is the diagonal matrix of pilots, \mathbf{R}_p is the corresponding received pilot signals, and \mathbf{F}_p is the $|\mathbf{J}| \times \kappa^{(j,i)}$ truncated DFT matrix over pilot subcarriers. Likewise, since the received pilot signals from different antenna pair do not interfere with each other, we can also perform the channel estimation o for each transceiver antenna pair. In order to initialize the channel estimator of (4.8), the CSI estimated in the last iteration of previous time slot has to be taken as the initial value of the CSI for the current time slot.



Then, we can construct an MMSE cost function over all subcarrier indices, and derive the minimum β as follows:

$$\begin{aligned} \beta &= \operatorname{argmin}_{\beta} E \left[\left\| \hat{\mathbf{H}}_v - \mathbf{H}_v \right\|^2 \right] \\ &= \operatorname{argmin}_{\beta} E \left[\left(\hat{\mathbf{H}}_v - \mathbf{H}_v \right)^* \left(\hat{\mathbf{H}}_v - \mathbf{H}_v \right) \right] \\ &= \operatorname{argmin}_{\beta} E \left[\hat{\mathbf{H}}_v^* \hat{\mathbf{H}}_v - \hat{\mathbf{H}}_v^* \mathbf{H}_v - \mathbf{H}_v^* \hat{\mathbf{H}}_v + \mathbf{H}_v^* \mathbf{H}_v \right] \\ &= \operatorname{argmin}_{\beta} f(\beta) \end{aligned} \quad (4.9)$$

where \mathbf{H}_v is the true value of current channel frequency response. Each component of $f(\beta)$ can be derived separately in the following. From (4.8) and (4.9), we have

$$\begin{aligned}
E[\hat{\mathbf{H}}_v^* \hat{\mathbf{H}}_v] &= E\left[\left((1-\beta)\hat{\mathbf{H}}_{v-1}^* + \beta\hat{\mathbf{H}}_p^*\right)\left((1-\beta)\hat{\mathbf{H}}_{v-1} + \beta\hat{\mathbf{H}}_p\right)\right] \\
&= E\left[(1-\beta)^2 \hat{\mathbf{H}}_{v-1}^* \hat{\mathbf{H}}_{v-1} + (1-\beta)\beta\hat{\mathbf{H}}_{v-1}^* \hat{\mathbf{H}}_p + \beta(1-\beta)\hat{\mathbf{H}}_p^* \hat{\mathbf{H}}_{v-1} + \beta^2 \hat{\mathbf{H}}_p^* \hat{\mathbf{H}}_p\right]
\end{aligned} \tag{4.10}$$

Let the estimation of \mathbf{H}_{v-1} be the summation of the true previous value plus a noise term, and the estimation of \mathbf{H}_p also be the summation of the true current value plus a noise term as follows:

$$\begin{aligned}
\hat{\mathbf{H}}_{v-1} &= \mathbf{H}_{v-1} + \tilde{\mathbf{Z}}_{v-1} \\
\hat{\mathbf{H}}_p &= \mathbf{H}_p + \tilde{\mathbf{Z}}_p
\end{aligned} \tag{4.11}$$

with

$$\begin{aligned}
\sigma_{\tilde{\mathbf{Z}}_{v-1}}^2 &= E[\tilde{\mathbf{Z}}_{v-1}^* \tilde{\mathbf{Z}}_{v-1}] \\
&= E\left[\left(\mathbf{F}(\mathbf{F}_d^H \mathbf{F}_d)^{-1} \mathbf{F}_d^H \mathbf{X}^{-1} \mathbf{Z}_{v-1}\right)^H \left(\mathbf{F}(\mathbf{F}_d^H \mathbf{F}_d)^{-1} \mathbf{F}_d^H \mathbf{X}^{-1} \mathbf{Z}_{v-1}\right)\right] \\
&= E\left[\left(\mathbf{W}_D \mathbf{X}^{-1} \mathbf{Z}_{v-1}\right)^H \left(\mathbf{W}_D \mathbf{X}^{-1} \mathbf{Z}_{v-1}\right)\right], \text{ where } \mathbf{W}_D = \mathbf{F}(\mathbf{F}_d^H \mathbf{F}_d)^{-1} \mathbf{F}_d^H \\
&= Tr\left\{E\left[\left(\mathbf{W}_D \mathbf{X}^{-1} \mathbf{Z}_{v-1}\right)\left(\mathbf{W}_D \mathbf{X}^{-1} \mathbf{Z}_{v-1}\right)^H\right]\right\} \\
&= Tr\left\{E\left[\mathbf{W}_D \mathbf{X}^{-1} \mathbf{Z}_{v-1} \mathbf{Z}_{v-1}^H \mathbf{X}^{-H} \mathbf{W}_D^H\right]\right\} \\
&= \frac{\sigma_z^2}{\sigma_s^2} Tr\left\{\mathbf{W}_D \mathbf{W}_D^H\right\} \\
&= \frac{N_0}{2E_b} Tr\left\{\mathbf{W}_D \mathbf{W}_D^H\right\}
\end{aligned} \tag{4.12}$$

and

$$\begin{aligned}
\sigma_{\tilde{\mathbf{Z}}_v}^2 &= E\left[\tilde{\mathbf{Z}}_v^* \tilde{\mathbf{Z}}_v\right] \\
&= E\left[\left(\mathbf{F}(\mathbf{F}_p^H \mathbf{F}_p)^{-1} \mathbf{F}_p^H \mathbf{X}_p^{-1} \mathbf{Z}_v\right)^H \left(\mathbf{F}(\mathbf{F}_p^H \mathbf{F}_p)^{-1} \mathbf{F}_p^H \mathbf{X}_p^{-1} \mathbf{Z}_v\right)\right] \\
&= E\left[\left(\mathbf{W}_p \mathbf{X}_p^{-1} \mathbf{Z}_v\right)^H \left(\mathbf{W}_p \mathbf{X}_p^{-1} \mathbf{Z}_v\right)\right], \text{ where } \mathbf{W}_p = \mathbf{F}(\mathbf{F}_p^H \mathbf{F}_p)^{-1} \mathbf{F}_p^H \\
&= \text{Tr}\left\{E\left[\left(\mathbf{W}_p \mathbf{X}_p^{-1} \mathbf{Z}_v\right)\left(\mathbf{W}_p \mathbf{X}_p^{-1} \mathbf{Z}_v\right)^H\right]\right\} \\
&= \text{Tr}\left\{E\left[\mathbf{W}_p \mathbf{X}_p^{-1} \mathbf{Z}_v \mathbf{Z}_v^H \mathbf{X}_p^{-H} \mathbf{W}_p^H\right]\right\} \\
&= \frac{\sigma_z^2}{\sigma_p^2} \text{Tr}\left\{\mathbf{W}_p \mathbf{W}_p^H\right\}, \text{ where } \sigma_p^2 \text{ is pilot power}
\end{aligned} \tag{4.13}$$

where $\text{Tr}\{\cdot\}$ denotes the trace of a square matrix.

Furthermore, the autocorrelation function of the channel frequency response is as follows:

$$\begin{aligned}
\mathbf{H}_{v-1} &= \mathbf{F} \mathbf{h}_{v-1} \\
\mathbf{H}_v &= \mathbf{F} \mathbf{h}_v \\
E\left[\mathbf{H}_v^* \mathbf{H}_v\right] &= E\left[\mathbf{h}_v^* \mathbf{F}^* \mathbf{F} \mathbf{h}_v\right] = E\left[\mathbf{h}_v^* \mathbf{h}_v\right] = \sigma_h^2 \\
E\left[\mathbf{H}_{v-1}^* \mathbf{H}_{v-1}\right] &= E\left[\mathbf{h}_{v-1}^* \mathbf{F}^* \mathbf{F} \mathbf{h}_{v-1}\right] = E\left[\mathbf{h}_{v-1}^* \mathbf{h}_{v-1}\right] = \sigma_h^2 \\
E\left[\mathbf{H}_{v-1}^* \mathbf{H}_v\right] &= E\left[\mathbf{h}_{v-1}^* \mathbf{F}^* \mathbf{F} \mathbf{h}_v\right] = E\left[\mathbf{h}_{v-1}^* \mathbf{h}_v\right] = \sigma_h^2 J_0(2\pi f_d T) \\
E\left[\mathbf{H}_v^* \mathbf{H}_{v-1}\right] &= E\left[\mathbf{h}_v^* \mathbf{F}^* \mathbf{F} \mathbf{h}_{v-1}\right] = E\left[\mathbf{h}_v^* \mathbf{h}_{v-1}\right] = \sigma_h^2 J_0(2\pi f_d T)
\end{aligned} \tag{4.14}$$

where $J_0(\cdot)$ denotes the zero-order Bessel function of the first kind, and f_d is Doppler frequency in hertz, σ_h^2 is the channel power, and T is the time duration of one OFDM symbol after adding the guard interval.

Hence, from (4.12) ~ (4.14), (4.10) is equivalent to

$$\begin{aligned}
E\left[\hat{\mathbf{H}}_v^* \hat{\mathbf{H}}_v\right] &= (1-\beta)^2 \left(E\left[\mathbf{H}_{v-1}^* \mathbf{H}_{v-1}\right] + E\left[\tilde{\mathbf{Z}}_{v-1}^* \tilde{\mathbf{Z}}_{v-1}\right]\right) + (1-\beta)\beta E\left[\mathbf{H}_{v-1}^* \mathbf{H}_v\right] \\
&\quad + \beta(1-\beta) E\left[\mathbf{H}_v^* \mathbf{H}_{v-1}\right] + \beta^2 \left(E\left[\mathbf{H}_v^* \mathbf{H}_v\right] + E\left[\tilde{\mathbf{Z}}_v^* \tilde{\mathbf{Z}}_v\right]\right) \\
&= (1-\beta)^2 \left(\sigma_h^2 + \sigma_{\tilde{\mathbf{Z}}_{v-1}}^2\right) + (1-\beta)\beta \sigma_h^2 J_0(2\pi f_d T) \\
&\quad + \beta(1-\beta) \sigma_h^2 J_0(2\pi f_d T) + \beta^2 \left(\sigma_h^2 + \sigma_{\tilde{\mathbf{Z}}_v}^2\right)
\end{aligned} \tag{4.15}$$

Similarly, we can obtain

$$\begin{aligned}
E[\hat{\mathbf{H}}_v^* \mathbf{H}_v] &= E\left[\left((1-\beta)\hat{\mathbf{H}}_{v-1}^* + \beta\hat{\mathbf{H}}_p^*\right)\mathbf{H}_v\right] \\
&= (1-\beta)E[\hat{\mathbf{H}}_{v-1}^* \mathbf{H}_v] + \beta E[\hat{\mathbf{H}}_p^* \mathbf{H}_v] \\
&= (1-\beta)E[\mathbf{H}_{v-1}^* \mathbf{H}_v] + \beta E[\mathbf{H}_v^* \mathbf{H}_v] \\
&= (1-\beta)\sigma_h^2 J_0(2\pi f_d T) + \beta\sigma_h^2
\end{aligned} \tag{4.16}$$

$$\begin{aligned}
E[\mathbf{H}_v^* \hat{\mathbf{H}}_v] &= E\left[\mathbf{H}_v^* \left((1-\beta)\hat{\mathbf{H}}_{v-1} + \beta\hat{\mathbf{H}}_p\right)\right] \\
&= (1-\beta)E[\mathbf{H}_v^* \hat{\mathbf{H}}_{v-1}] + \beta E[\mathbf{H}_v^* \hat{\mathbf{H}}_p] \\
&= (1-\beta)E[\mathbf{H}_v^* \mathbf{H}_{v-1}] + \beta E[\mathbf{H}_v^* \mathbf{H}_v] \\
&= (1-\beta)\sigma_h^2 J_0(2\pi f_d T) + \beta\sigma_h^2
\end{aligned} \tag{4.17}$$

Therefore, apply (4.15)~(4.17) into (4.9) then we can get the following equation:

$$\begin{aligned}
\beta &= \arg \min_{\beta} f(\beta) \\
&= \arg \min_{\beta} \left[(1-\beta)^2 (\sigma_h^2 + \sigma_{\hat{\mathbf{z}}_{v-1}}^2) + (1-\beta)\beta\sigma_h^2 J_0(2\pi f_d T) + \beta(1-\beta)\sigma_h^2 J_0(2\pi f_d T) + \beta^2 (\sigma_h^2 + \sigma_{\hat{\mathbf{z}}_v}^2) \right. \\
&\quad \left. - (1-\beta)\sigma_h^2 J_0(2\pi f_d T) - \beta\sigma_h^2 - (1-\beta)\sigma_h^2 J_0(2\pi f_d T) - \beta\sigma_h^2 + \sigma_h^2 \right] \\
&= \arg \min_{\beta} \left[(2\sigma_h^2 + \sigma_{\hat{\mathbf{z}}_{v-1}}^2 - 2\sigma_h^2 J_0(2\pi f_d T) + \sigma_{\hat{\mathbf{z}}_v}^2) \beta^2 + (-4\sigma_h^2 - 2\sigma_{\hat{\mathbf{z}}_{v-1}}^2 + 4\sigma_h^2 J_0(2\pi f_d T)) \beta \right. \\
&\quad \left. + (2\sigma_h^2 + \sigma_{\hat{\mathbf{z}}_{v-1}}^2 - 2\sigma_h^2 J_0(2\pi f_d T)) \right]
\end{aligned} \tag{4.18}$$

By taking $\frac{\partial f(\beta)}{\partial \beta} = 0$, the optimum value of β is given by

$$\beta = \frac{2\sigma_h^2 + \sigma_{\hat{\mathbf{z}}_{v-1}}^2 - 2\sigma_h^2 J_0(2\pi f_d T)}{2\sigma_h^2 + \sigma_{\hat{\mathbf{z}}_{v-1}}^2 - 2\sigma_h^2 J_0(2\pi f_d T) + \sigma_{\hat{\mathbf{z}}_v}^2} \tag{4.19}$$

We can observe from the above equation that as the mobile speed is slow, $J_0(2\pi f_d T) \approx 1$

and then $\beta \approx \frac{\sigma_{\hat{\mathbf{z}}_{v-1}}^2}{\sigma_{\hat{\mathbf{z}}_{v-1}}^2 + \sigma_{\hat{\mathbf{z}}_v}^2}$; as the mobile speed is fast, $J_0(2\pi f_d T) \approx 0$ and $\beta \approx 1$.

It is noted that, after the first iteration, we execute the channel tracking process of (4.7) for the second and subsequent iterations until a stopping criterion holds. The stopping criterion is to check whether the iteration number ν reaches the maximum value of V . The channel

tracking process for the current time slot will be stopped when the above condition holds.

Fig.4 outlines the β -tracker followed by DF DFT-based channel estimation method to estimate the average channel variations in the tracking stage. We perform the channel estimator described above for each transceiver antenna pair respectively, and then after each iteration we have $\hat{\mathbf{H}}_v^{(j,i)} = \langle \hat{H}_v^{(j,i)}[k, k] : k \in \Omega = \{0, \dots, N-1\} \rangle$ for $i = 1, \dots, N_T$ and $j = 1, \dots, N_R$. With the knowledge of $\hat{H}_v^{(j,i)}[k, k]$ for $i = 1, \dots, N_T$ and $j = 1, \dots, N_R$, we can detect data by performing V-BLAST with MMSE-SIC algorithm on each subcarrier as mentioned in chapter 3.

For $1 \leq v \leq V$

For each antenna pair (j, i) where $1 \leq j \leq N_R, 1 \leq i \leq N_T$

 If $v = 1$

$\hat{\mathbf{H}}_v = (1 - \beta) \hat{\mathbf{H}}_{v-1} + \beta \hat{\mathbf{H}}_p$

 where $\hat{\mathbf{H}}_p = \mathbf{F} (\mathbf{F}_p^H \mathbf{F}_p)^{-1} \mathbf{F}_p^H \mathbf{X}_p^{-1} \mathbf{R}_p$

 else

$\hat{\mathbf{H}}_v = \mathbf{F} (\mathbf{F}_d^H \mathbf{F}_d)^{-1} \mathbf{F}_d^H \hat{\mathbf{X}}^{-1} \tilde{\mathbf{R}}_v$

 where $\tilde{\mathbf{R}}_v^{(j,i)} = \langle \tilde{R}_v^{(j,i)}[k] = R^{(j)}[k] - \sum_{m \neq i} \hat{H}^{(j,m)}[k, k] \hat{X}^{(m)}[k], k \in \Theta \rangle$

 End

End

We can get $\hat{\mathbf{H}}_v^{(j,i)} = \langle \hat{H}_v^{(j,i)}[k, k] : k \in \Omega = \{0, \dots, N-1\} \rangle$

Detect data using V-BLAST with MMSE-SIC algorithm: $\hat{\mathbf{X}}$

Assign $v = v + 1$

End

Assign $\hat{\mathbf{H}}_0 = \hat{\mathbf{H}}_v$

Fig. 5 β -tracker followed by DF DFT-based channel estimation method in the tracking stage

4.3 ICI Estimation

In the presence of Doppler caused by high mobility, due to the ICI term of (2.8), using the estimate of average channel for data detection results in poor performance. This motivates the need to perform ICI estimation.

In this stage, we adopt a linear model with a constant slope over the time duration of one OFDM symbol to approximate time variations of each path. When the linear model is applied, we will derive the frequency domain relationship, similar to (2.8). We first consider the SISO case with one transmit and one receive antenna by omitting the superscript “ (j, i) ” and “ (i) ”, and in the end of this section we will apply it to MIMO case.

The received signal of SISO case is as follows:

$$\begin{aligned}
 Y[k] &= \sum_{m=0}^{N-1} X[m]H[k, m] + Z[k] \\
 &= X[k]H[k, k] + \underbrace{\sum_{m=0, m \neq k}^{N-1} X[m]H[k, m]}_{\text{ICI}} + Z[k]
 \end{aligned} \tag{4.20}$$

where $X[k]$ is transmitted symbols which we assume it is known, and $H[k, m]$ denotes the channel frequency response from the m th subcarrier on the k th one which can be expressed as:

$$H[k, m] = \sum_{l=0}^{L-1} \left[\frac{1}{N} \sum_{n=0}^{N-1} h_l[n] e^{-\frac{j2\pi n(k-m)}{N}} \right] e^{-\frac{j2\pi m\tau_l}{N}}. \tag{4.21}$$

Furthermore, we assume $H[k, k]$ is known which can be obtained from β -tracker and can be expressed as

$$H[k, k] = \sum_{l=0}^{L-1} \mu_{l,0} e^{-\frac{j2\pi k \tau_l}{N}} \quad (4.22)$$

where $\mu_{l,0}$ is the average channel variation of the l th path. Through an IDFT, we have

$$\mu_{l,0} = \sum_{k=0}^{N-1} H[k, k] e^{\frac{j2\pi k \tau_l}{N}} \quad 0 \leq l \leq L-1. \quad (4.23)$$

Let $\mu_{l,1}$ denote the slope of the l th path in the current OFDM symbol. To perform the linearization, knowledge of the channel at one time instant in the symbol is necessary. As mentioned in [7], let $E[z]$ represent the average of z . Then for the l th channel tap, $E\left[\left|\mu_{l,0} - h_l[n]\right|^2\right]$ is minimized for $n = \left(\frac{N}{2} - 1\right)$. Therefore, we approximate $h_l\left[\frac{N}{2} - 1\right]$

with $\mu_{l,0}$. We will have

$$\hat{h}_l\left[\frac{N}{2} - 1\right] = \mu_{l,0}. \quad (4.24)$$

Consider linearization around $h_l\left[\frac{N}{2} - 1\right]$. Then, $h_l[n]$ can be approximated as follows:

$$h_l[n] = \mu_{l,1} \left(n - \frac{N}{2} + 1\right) + \mu_{l,0} \quad 0 \leq n \leq N-1 \quad (4.25)$$

Inserting (4.25) into (4.21), we will have

$$H[k, m] = \sum_{l=0}^{L-1} \left\{ \frac{1}{N} \sum_{n=0}^{N-1} \left[\mu_{l,1} \left(n - \frac{N}{2} + 1\right) + \mu_{l,0} \right] e^{-\frac{j2\pi n(k-m)}{N}} \right\} e^{-\frac{j2\pi m \tau_l}{N}} \quad 0 \leq k, m \leq N-1 \quad (4.26)$$

Subtract the non-ICI term from the received signals $Y[k]$ and we will have $\tilde{R}[k]$ as follows:

$$\tilde{R}[k] = Y[k] - X[k]H[k, k] = \sum_{m=0, m \neq k}^{N-1} X[m]H[k, m] + Z[k] \quad (4.27)$$

Then we can construct an ML cost function and the slope of each path $\mu_{l,1}$ can be found by minimizing the following cost function:

$$\begin{aligned}
\mu_{l,1} &= \arg \min_{\mu_{l,1}} \sum_{k \in \Theta} \left| \tilde{R}[k] - \sum_{m=0, m \neq k}^{N-1} X[m] H[k, m] \right|^2 \\
&= \arg \min_{\mu_{l,1}} \sum_{k \in \Theta} \left| \tilde{R}[k] - \sum_{m=0, m \neq k}^{N-1} X[m] \left(\sum_{l=0}^{L-1} \left\{ \frac{1}{N} \sum_{n=0}^{N-1} \left[\mu_{l,1} \left(n - \frac{N}{2} + 1 \right) + \mu_{l,0} \right] e^{-\frac{j2\pi n(k-m)}{N}} \right\} e^{-\frac{j2\pi m \tau_l}{N}} \right) \right|^2 \\
&= \arg \min_{\mu_{l,1}} \sum_{k \in \Theta} \left| \tilde{R}[k] - \sum_{m=0, m \neq k}^{N-1} X[m] \left\{ \sum_{l=0}^{L-1} \mu_{l,1} \left[\frac{1}{N} \sum_{n=0}^{N-1} \left(n - \frac{N}{2} + 1 \right) e^{-\frac{j2\pi n(k-m)}{N}} \right] e^{-\frac{j2\pi m \tau_l}{N}} \right\} \right. \\
&\quad \left. - \sum_{m=0, m \neq k}^{N-1} X[m] \left[\sum_{l=0}^{L-1} \mu_{l,0} \left(\frac{1}{N} \sum_{n=0}^{N-1} e^{-\frac{j2\pi n(k-m)}{N}} \right) e^{-\frac{j2\pi m \tau_l}{N}} \right] \right|^2 \\
&= \arg \min_{\mu_{l,1}} \sum_{k \in \Theta} \left| \tilde{R}[k] - \sum_{m=0, m \neq k}^{N-1} X[m] \left[\sum_{l=0}^{L-1} \mu_{l,1} \left(\frac{1}{N} \sum_{n=0}^{N-1} n e^{-\frac{j2\pi n(k-m)}{N}} \right) e^{-\frac{j2\pi m \tau_l}{N}} \right] \right|^2 \\
&\quad \left(\because \text{for } m \neq k, \frac{1}{N} \sum_{n=0}^{N-1} e^{-\frac{j2\pi n(k-m)}{N}} = 0 \right)
\end{aligned} \tag{4.28}$$

For simplification, let

$$\frac{1}{N} \sum_{n=0}^{N-1} n e^{-\frac{j2\pi n(k-m)}{N}} = a[k, m] \tag{4.29}$$

and we can modify the cost function as

$$\begin{aligned}
f(\mu_{l,1}) &= \sum_{k \in \mathcal{J}} \left| \tilde{R}[k] - \sum_{m=0, m \neq k}^{N-1} X[m] \left[\sum_{l=0}^{L-1} \mu_{l,1} \left(\frac{1}{N} \sum_{n=0}^{N-1} n e^{-\frac{j2\pi n(k-m)}{N}} \right) e^{-\frac{j2\pi m \tau_l}{N}} \right] \right|^2 \\
&= \sum_{k \in \mathcal{J}} \left| \tilde{R}[k] - \sum_{m=0, m \neq k}^{N-1} X[m] \left[\sum_{l=0}^{L-1} \mu_{l,1} a[k, m] e^{-\frac{j2\pi m \tau_l}{N}} \right] \right|^2
\end{aligned} \tag{4.30}$$

Hence, $\mu_{l,1}$ can be determined by

$$\frac{\partial f(\mu_{l,1})}{\partial \mu_{l,1}} \triangleq \frac{1}{2} \left\{ \frac{\partial f(\mu_{l,1})}{\partial \text{Re}(\mu_{l,1})} - j \frac{\partial f(\mu_{l,1})}{\partial \text{Im}(\mu_{l,1})} \right\} = 0 \tag{4.31}$$

Direct calculation yields that (4.31) is equivalent to

$$\sum_{k \in \mathcal{J}} \left(\tilde{R}[k] - \sum_{m=0, m \neq k}^{N-1} X[m] \left[\sum_{l=0}^{L-1} \mu_{l,1} a[k, m] e^{-\frac{j2\pi m \tau_l}{N}} \right] \right) \cdot \sum_{m=0, m \neq k}^{N-1} X^*[m] a^*[k, m] e^{\frac{j2\pi m \tau_l}{N}} = 0 \tag{4.32}$$

for $l' = 0, 1, \dots, L-1$.

Now we define

$$\sum_{k \in \mathbf{J}} \tilde{R}[k] \sum_{m=0, m \neq k}^{N-1} X^*[m] a^*[k, m] e^{\frac{j2\pi m \tau_l}{N}} = b[l'] \quad (4.33)$$

and

$$\sum_{k \in \mathbf{J}} \sum_{m=0, m \neq k}^{N-1} X[m] a[k, m] e^{-\frac{j2\pi m \tau_l}{N}} \sum_{m=0, m \neq k}^{N-1} X^*[m] a^*[k, m] e^{\frac{j2\pi m \tau_l}{N}} = q[l, l'] \quad (4.34)$$

Then, (4.32) is equivalent to

$$\sum_{l=0}^{L-1} \mu_{l,1} q[l, l'] = b[l'] \quad 0 \leq l' \leq L-1 \quad (4.35)$$

Equation (4.35) can be written in matrix form as

$$\mathbf{Q} \mathbf{m} = \mathbf{b} \quad (4.36)$$

where $\mathbf{Q} = \begin{pmatrix} q[0,0] & q[1,0] & \cdots & q[L-1,0] \\ q[0,1] & q[1,1] & \cdots & q[L-1,1] \\ \vdots & \vdots & \ddots & \vdots \\ q[0,L-1] & q[1,L-1] & \cdots & q[L-1,L-1] \end{pmatrix}$, $\mathbf{m} = \begin{pmatrix} \mu_{0,1} \\ \mu_{1,1} \\ \vdots \\ \mu_{L-1,1} \end{pmatrix}$, and $\mathbf{b} = \begin{pmatrix} b[0] \\ b[1] \\ \vdots \\ b[L-1] \end{pmatrix}$.

Hence, the slope of each path can be estimated by

$$\mathbf{m} = \mathbf{Q}^{-1} \mathbf{b} \quad (4.37)$$

and with the knowledge of the slope of each path, we can reconstruct the channel frequency response $H[k, m]$ as shown in (4.26).

Now, with the ICI estimation for SISO case, we can apply it to MIMO case by modifying the received signal $Y[k]$ in (4.20) and perform the ICI estimation for each antenna pair. In MIMO environment, received signal at each receive antenna suffers from inter-antenna interference including intercarrier interference (ICI) as follows:

$$\begin{aligned}
R^{(j)}[k] &= \sum_{i=1}^{N_r} \sum_{m=0}^{N-1} H^{(j,i)}[k,m] X^{(i)}[m] + Z^{(j)}[k] \\
&= \sum_{i=1}^{N_r} \left(H^{(j,i)}[k,k] X^{(i)}[k] + \underbrace{\sum_{m=0, m \neq k}^{N-1} H^{(j,i)}[k,m] X^{(i)}[m]}_{ICI} \right) + Z^{(j)}[k]
\end{aligned} \tag{4.38}$$

To let the received signal in MIMO case corresponding to the (j,i) th antenna pair, named it as refined signal, be the same as $Y[k]$ in SISO case, we need to subtract the inter-antenna interference including ICI from the received signal $R^{(j)}[k]$ as follows:

$$\begin{aligned}
\widehat{R}^{(j,i)}[k] &= R^{(j)}[k] - \sum_{n \neq i} \sum_{m=0}^{N-1} H^{(j,n)}[k,m] X^{(n)}[k] \\
&= \sum_{m=0}^{N-1} H^{(j,i)}[k,m] X^{(i)}[m] + Z[k] \\
&= H^{(j,i)}[k,k] X^{(i)}[k] + \underbrace{\sum_{m=0, m \neq k}^{N-1} H^{(j,i)}[k,m] X^{(i)}[m]}_{ICI} + Z[k]
\end{aligned} \tag{4.39}$$

Then the refined signal $\widehat{R}^{(j,i)}[k]$ which is only the received signal between the “ (j,i) ” antenna pair can be treated as $Y[k]$ in SISO case. However, in the beginning of this stage, $H^{(j,n)}[k,m]$ is not available, so we cannot obtain $\widehat{R}^{(j,i)}[k]$. Therefore, with the simulation in the following, we use another refined signal $\widetilde{R}^{(j,i)}[k]$ which is obtained by subtracting inter-antenna interference excluding ICI term from the received signal $R^{(j)}[k]$ as follows to estimate the slope of each path:

$$\widetilde{R}^{(j,i)}[k] = R^{(j)}[k] - \sum_{n \neq i} H^{(j,n)}[k,k] X^{(n)}[k]. \tag{4.40}$$

In the following simulation, we assume that average channel variations $\mu_{l,0}^{(j,i)}$ are known and inter-antenna interference excluding ICI can be perfectly subtracted from received signal $R^{(j)}[k]$. We adopt the refined signal $\widetilde{R}^{(j,i)}[k]$, and perform ICI estimation to estimate the

slope of each path for each antenna pair, and then we have

$$\hat{h}_l^{(j,i)}[n] = \mu_{l,1}^{(j,i)} \left(n - \frac{N}{2} + 1 \right) + \mu_{l,0}^{(j,i)} \quad 0 \leq n \leq N-1 \quad (4.41)$$

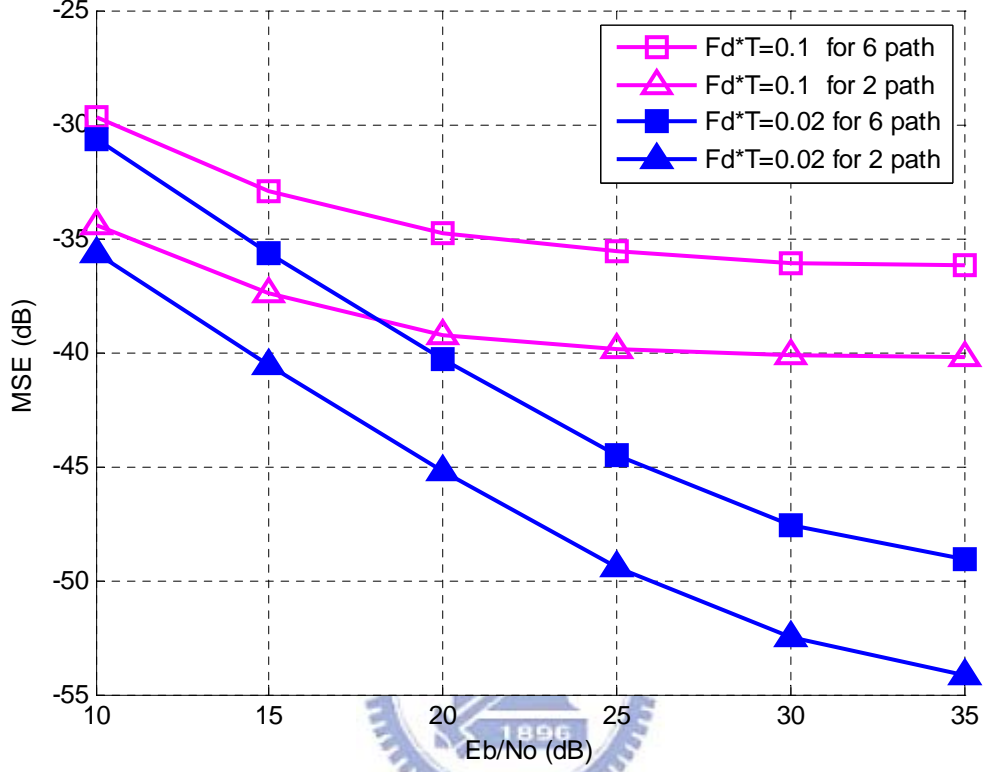


Fig. 6 NMSE of the channel estimation with the assumption that the average channel

variations $\mu_{l,0}^{(j,i)}$ for $l = 0, \dots, L^{(j,i)}$ are known versus E_b / N_o

Fig. 6 shows the normalized mean square error (NMSE) of channel estimation with the assumption that the average channel variations $\mu_{l,0}^{(j,i)}$ for $l = 0, \dots, L^{(j,i)}$ are known by using refined signal $\tilde{R}^{(j,i)}[k]$ in the two- path and six-path channel for normalized Doppler frequency $f_d \cdot T$ equals to 0.02 and 0.1, respectively. As can be observed in Fig. 6, the MSE of channel variations are all quite small even in low E_b / N_o region. Hence, to perform ICI estimation for MIMO case, we just need to modify (4.20) as follows:

$$Y[k] = \tilde{R}^{(j,i)}[k] = R^{(j)}[k] - \sum_{n \neq i} H^{(j,n)}[k,k] X^{(n)}[k] \quad (4.42)$$

In the above derivation, we have assumed that the transmitted signals for each antenna are known. However, in reality, the transmitted signals are obtained by applying the V-BLAST detection as shown in chapter 3 to received signals.

4.4 Two Dimensional V-BLAST Detection

In section 2.4, we have known that the ICI effect on OFDM systems and its mathematic representation. Now, we change the mathematic representation in section 2.4 into matrix form which is convenient to be used in this section.

Define $\mathbf{R}^{(j)} = \langle R^{(j)}[0], \dots, R^{(j)}[N-1] \rangle$, $\mathbf{R} = \langle \mathbf{R}^{(1)}, \dots, \mathbf{R}^{(N_R)} \rangle$,

$\mathbf{X}^{(i)} = \langle X^{(i)}[0], \dots, X^{(i)}[N-1] \rangle$, $\mathbf{X} = \langle \mathbf{X}^{(1)}, \dots, \mathbf{X}^{(N_T)} \rangle$,

$$\mathbf{H}^{(j,i)} = \begin{bmatrix} H^{(j,i)}[0,0] & \dots & H^{(j,i)}[0,N-1] \\ \vdots & \ddots & \vdots \\ H^{(j,i)}[N-1,0] & \dots & H^{(j,i)}[N-1,N-1] \end{bmatrix}, \text{ and } \mathbf{H} = \begin{bmatrix} \mathbf{H}^{(1,1)} & \dots & \mathbf{H}^{(1,N_T)} \\ \vdots & \ddots & \vdots \\ \mathbf{H}^{(N_R,1)} & \dots & \mathbf{H}^{(N_R,N_T)} \end{bmatrix}.$$

Then the received signals \mathbf{R} suffer not only from inter-antenna interference but also from intercarrier interference and (2.8) can be expressed as follows:

$$\mathbf{R} = \mathbf{H}\mathbf{X} + \mathbf{Z} \quad (4.43)$$

In this section a two-dimensional V-BLAST method is utilized to perform ICI cancellation and data detection. From [13], we know that most of the ICI effect on a subcarrier comes from neighboring subcarriers, so we assume the group size of the ICI effect is $A = 2a + 1$

which means that $X^{(i)}[n]$ causes interference to $R^{(j)}[\left((n-a)\right)_N] \sim R^{(j)}[\left((n+a)\right)_N]$ for $j=1, \dots, N_R$. Let $\mathbf{S}_n^{(i)} = \langle X^{(i)}[n \cdot A], \dots, X^{(i)}[(n+1)A-1] \rangle$ be a segment of $\mathbf{X}^{(i)}$, $\mathbf{Y}_n^{(j)} = \langle R^{(j)}[n \cdot A], \dots, R^{(j)}[(n+1)A-1] \rangle$ be a segment of $\mathbf{R}^{(j)}$, and for any $n \neq m$, $\mathbf{S}_n^{(i)} \cap \mathbf{S}_m^{(i)} = \{0\}$ and $\mathbf{Y}_n^{(j)} \cap \mathbf{Y}_m^{(j)} = \{0\}$ where A is the size of one segment which is the same as the group size of the ICI effect. Accordingly, $\mathbf{S}_n^{(i)}$ will induce the interference on $\mathbf{Y}_{n-1}^{(j)}$, $\mathbf{Y}_n^{(j)}$, and $\mathbf{Y}_{n+1}^{(j)}$ for $j=1, \dots, N_R$. As shown in Fig.7, $\mathbf{Y}_n^{(j)}$ suffers the interference from $\mathbf{S}_{n-1}^{(i)}$, $\mathbf{S}_n^{(i)}$ and $\mathbf{S}_{n+1}^{(i)}$ or even more segments for $i=1, \dots, N_T$, so performance of solving $\mathbf{S}_n^{(i)}$ by $\mathbf{Y}_n^{(j)}$ directly may not be acceptable.

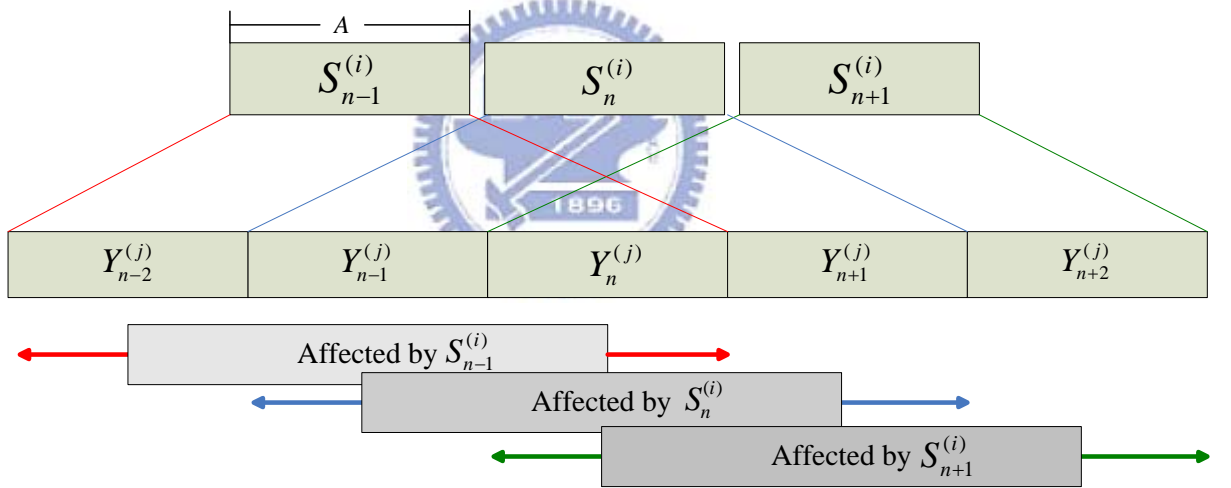


Fig. 7 ICI effect from neighboring subcarriers with group size A

The basic idea here is to cancel the component of $\mathbf{S}_m^{(i)} \sim \mathbf{S}_m^{(N_T)}$, $n \neq m$ in $\mathbf{Y}_n^{(j)}$. And treat the ICI effect in $\mathbf{Y}_n^{(j)}$ as inter-antenna interference in another dimension. Again, from [8], most of the ICI effect on a subcarrier comes from neighboring subcarriers. So $\mathbf{Y}_n^{(j)}$ is affected by $\mathbf{S}_{n-1}^{(i)}$, $\mathbf{S}_n^{(i)}$ and $\mathbf{S}_{n+1}^{(i)}$, and the relationship of them can be represented as follows:

$$\mathbf{Y}_n^{(j)} = \sum_{i=1}^{N_T} \left(\mathbf{H}_{n,n-1}^{(j,i)} \mathbf{S}_{n-1}^{(i)} + \mathbf{H}_{n,n}^{(j,i)} \mathbf{S}_n^{(i)} + \mathbf{H}_{n,n+1}^{(j,i)} \mathbf{S}_{n+1}^{(i)} \right) \quad (4.44)$$

where $\mathbf{H}_{n,m}^{(j,i)}$ is a block of $\mathbf{H}^{(j,i)}$ denoted as

$$\mathbf{H}_{n,m}^{(j,i)} = \begin{bmatrix} \mathbf{H}^{(j,i)} \left[\left((n \cdot A) \right)_N, \left((m \cdot A) \right)_N \right] & \cdots & \mathbf{H}^{(j,i)} \left[\left((n \cdot A) \right)_N, \left(((m+1)A-1) \right)_N \right] \\ \vdots & \ddots & \vdots \\ \mathbf{H}^{(j,i)} \left[\left(((n+1)A-1) \right)_N, \left((m \cdot A) \right)_N \right] & \cdots & \mathbf{H}^{(j,i)} \left[\left(((n+1)A-1) \right)_N, \left(((m+1)A-1) \right)_N \right] \end{bmatrix} \quad (4.45)$$

From section 4.2, we have solved $\hat{\mathbf{X}}$ by using V-BLAST detection. Now, we use the result $\hat{\mathbf{X}} = \langle \hat{\mathbf{X}}^{(1)}, \dots, \hat{\mathbf{X}}^{(N_T)} \rangle$ to do ICI cancellation by following equation:

$$\tilde{\mathbf{Y}}_n^{(j)} = \mathbf{Y}_n^{(j)} - \sum_{i=1}^{N_T} \left(\mathbf{H}_{n,n-1}^{(j,i)} \mathbf{S}_{n-1}^{(i)} + \mathbf{H}_{n,n+1}^{(j,i)} \mathbf{S}_{n+1}^{(i)} \right) \quad (4.46)$$

The ICI effect comes from $\mathbf{S}_{n-1}^{(i)}$ and $\mathbf{S}_{n+1}^{(i)}$ for $i=1, \dots, N_T$ in $\tilde{\mathbf{Y}}_n^{(j)}$ have been cleaned, and we can treat the remainder ICI effect in $\tilde{\mathbf{Y}}_n^{(j)}$ as inter-antenna interference in another

dimension. Then using $\langle \tilde{\mathbf{Y}}_n^{(1)}, \dots, \tilde{\mathbf{Y}}_n^{(N_T)} \rangle$ and $\begin{bmatrix} \mathbf{H}_{n,n}^{(1,1)} & \cdots & \mathbf{H}_{n,n}^{(1,N_T)} \\ \vdots & \ddots & \vdots \\ \mathbf{H}_{n,n}^{(N_T,1)} & \cdots & \mathbf{H}_{n,n}^{(N_T,N_T)} \end{bmatrix}$ to do V-BLAST

detection, which we call it as two-dimensional V-BLAST data detection, we can expect that

the more accurate $\mathbf{S}_n^{(1)} \sim \mathbf{S}_n^{(N_T)}$ can be obtained. Using the procedure described above

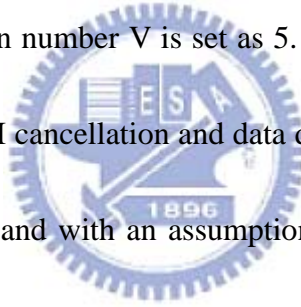
iteratively, we expect that the recovery performance will be better.

Chapter 5 Performance Simulation

5.1 System Parameters

Simulations are carried out for the proposed iterative receiver architecture. We consider a MIMO OFDM system with two transmit antennas and two receive antennas. The carrier frequency is 2.5 GHz and the system occupies a bandwidth of 5 MHz. OFDM effectively divides the entire bandwidth into $N = 256$ subcarriers among which $|\mathbf{Q}| + |\mathbf{J}| = 200$ subcarriers are used to transmit data symbols and pilot tones respectively, while pilot tones are alternatively inserted into the available pilot subcarriers to avoid inter-antenna interference at the receiver side. The subcarrier indices of pilot subcarriers are uniformly assigned within the available subcarriers. And the rest 56 subcarriers are used as either a DC subcarrier or virtual subcarriers at the two edges. In the simulation, the QPSK modulation scheme is adopted for the data symbols, and the pilot tones use the BPSK modulation scheme. Each pilot subcarrier transmits the same power as each data subcarrier. The length of the CP is 64 sample periods, i.e., one quarter of the useful symbol time. Each OFDM frame starts with a CP-added preamble which occupies one OFDM symbol and is followed by 50 consecutive OFDM data symbols. In order to avoid the preambles transmitted from different antennas interfering with each other at the receiver, the preambles transmitted from the first and second antennas utilize even and odd subcarriers respectively with a 3 dB power boost, and the values of those subcarriers are set according to [14]. Both a conventional two-path channel and an

International Telecommunication Union (ITU) Veh-B channel are simulated with the relative path power profiles set as 0, 0 (dB) for the two-path channel and -2.5, 0, -12.8, -10, -25.2, -16 (dB) for the ITU Veh-B channel [15], where the delay of the first path set as 0 and the others are uniformly distributed from 1 to τ_{MAX} (<64 sample periods). The system performance is demonstrated with normalized Doppler frequency $F_d * T$ equals to 0.02 \cdot 0.05 on mobile radio environments, for which Rayleigh fading is generated by Jakes' model [16]. The multipath observation window \mathbf{W}_b is set as [0,108] and the presumed number of paths N_p is set as 4 and 8 for the two-path channel and the ITU Veh-B channel. In the tracking stage, the value of the maximum iteration number V is set as 5. In the final stage, the group size of ICI effect is set as 5 to perform ICI cancellation and data detection. The entire simulations are conducted in the equivalent baseband with an assumption that both symbol synchronization and carrier synchronization are perfect. Finally, through the simulation, the parameter E_b / N_o is defined as a ratio of received bit energy to the power spectral density of noise.



5.2 Simulation Results

In the simulations, we demonstrate the performance of the proposed channel estimation methods with two methods as described in the following. Method I performs channel initialization and channel tracking, then detect data by conventional V-BLAST detection; Method II performs channel initialization, channel tracking, and ICI estimation and

cancellation with two-dimensional V-BLAST detection.

For comparison purpose, two performance curves with ideal channel estimation are provided for reference and served as performance lower bounds in each simulation figure. One of the performance curves is the ideal channel estimation with the assumption of that channel is quasi-static in one OFDM symbol duration, which is the simulation giving the midpoint of fading patterns of each path, and it is the performance lower bound of performing the method I, denoted as one tap equalizer (perfect CSI); the other is the ideal channel estimation with the knowledge of all fading patterns, which is the performance lower bound of performing the method II, represented as 2-D V-BLAST (perfect CSI).

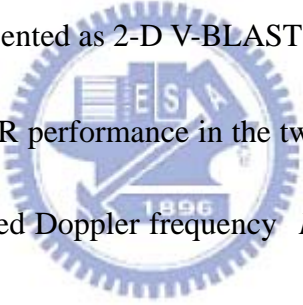


Fig. 8 and Fig. 9 shows the BER performance in the two-path channel and the ITU Veh-B channel, respectively, for normalized Doppler frequency $F_d * T = 0.02$. As can be observed in Fig. 8 and Fig. 9, the performance of the method I can almost achieve the performance curve of one tap equalizer with ideal channel estimation. However, an error floor is visible when SNR is high, which is due to the ICI effect resulting from channel variations. Method II which performs ICI cancellation can eliminate the phenomenon of error floor and achieve the performance lower bound of 2-D V-BLAST (perfect CSI). In Fig. 9, there is only 1dB degradation in the required E_b / N_o for method II at $BER = 10^{-3}$ compared with the performance curve of the 2-D V-BLAST (perfect CSI).

Fig.10 and Fig.11 shows the BER performance in the two-path channel and the ITU

Veh-B channel, respectively, for normalized Doppler frequency $F_d * T = 0.05$. As shown in Fig. 10, at $\text{BER} = 10^{-3}$, the required E_b / N_o for the method II is about 5dB less than that for the method I, and only 0.6dB degradation compared with the performance curve of the 2-D V-BLAST (perfect CSI). Similarly to the above results, the performance of method I can almost achieve the performance curve of one tap equalizer (perfect CSI) with slightly degradation in the required E_b / N_o . As the SNR is high, an error floor is clearly visible. Then with ICI cancellation, the method II significantly outperforms the method I. In Fig. 11, with ICI cancellation, the method II also provides a substantial gain in E_b / N_o , whereas it has 2dB gap in E_b / N_o compared with the 2-D V-BLAST (perfect CSI).

Fig. 12 shows the BER versus normalized Doppler frequency $F_d * T$ in the two-path channel at $E_b / N_o = 25\text{dB}$. Clearly, the BER performance gap between the method I and the method II becomes larger as normalized Doppler frequency increases up to 0.07. But as the normalized Doppler frequency increases higher, the gap between the method II and 2-D V-BLAST with perfect CSI becomes larger too. As the normalized Doppler frequency increases, the linear model for ICI estimation might not be enough to estimate the channel variations.

Fig. 13 and Fig. 14 show the BER performance in the two-path channel and the ITU Veh-B channel for normalized Doppler frequency $F_d * T = 0.05$ with different group size. We can observe that with greater group size, the BER performance gets better. Fig. 13 shows that

in the two-path channel with group size = 7, the BER performance can achieve the performance curve of the 2-D V-BLAST (perfect CSI). In Fig. 14, with greater group size, the BER performance also gets better, but the improvement of BER performance becomes smaller. We can also observe that with the *ici* iteration equals two, which performs ICI estimation and cancellation iteratively, the BER performance gets better too.



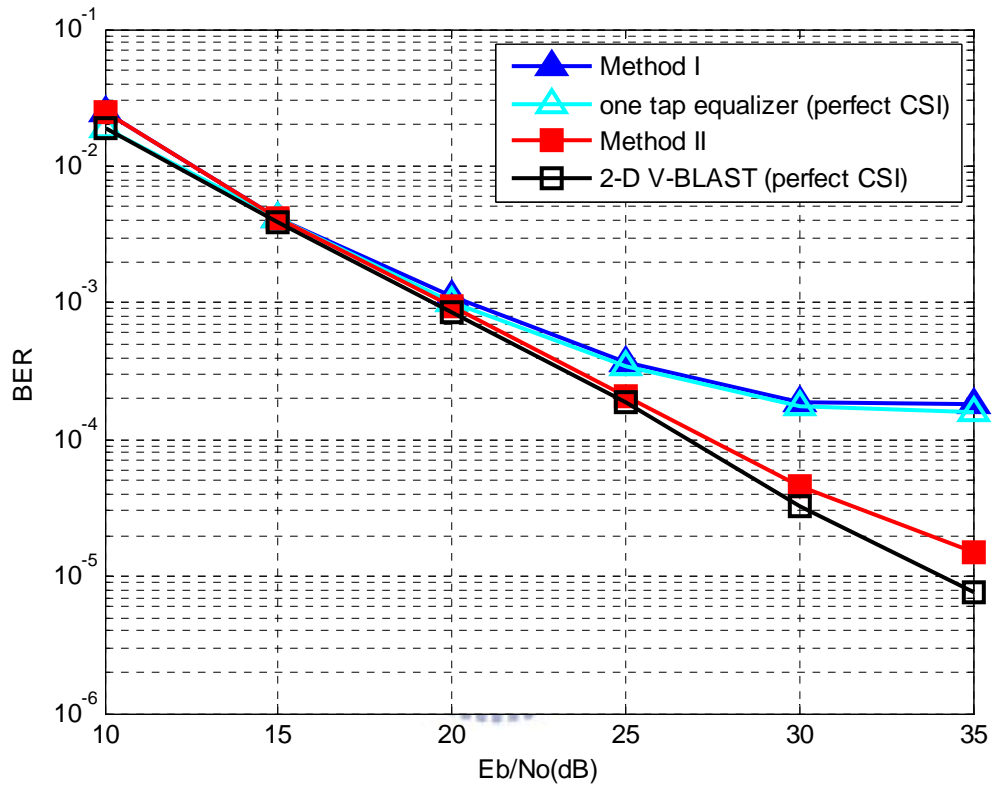


Fig. 8 BER performance in the two-path channel for normalized Doppler frequency

$$F_d * T = 0.02$$

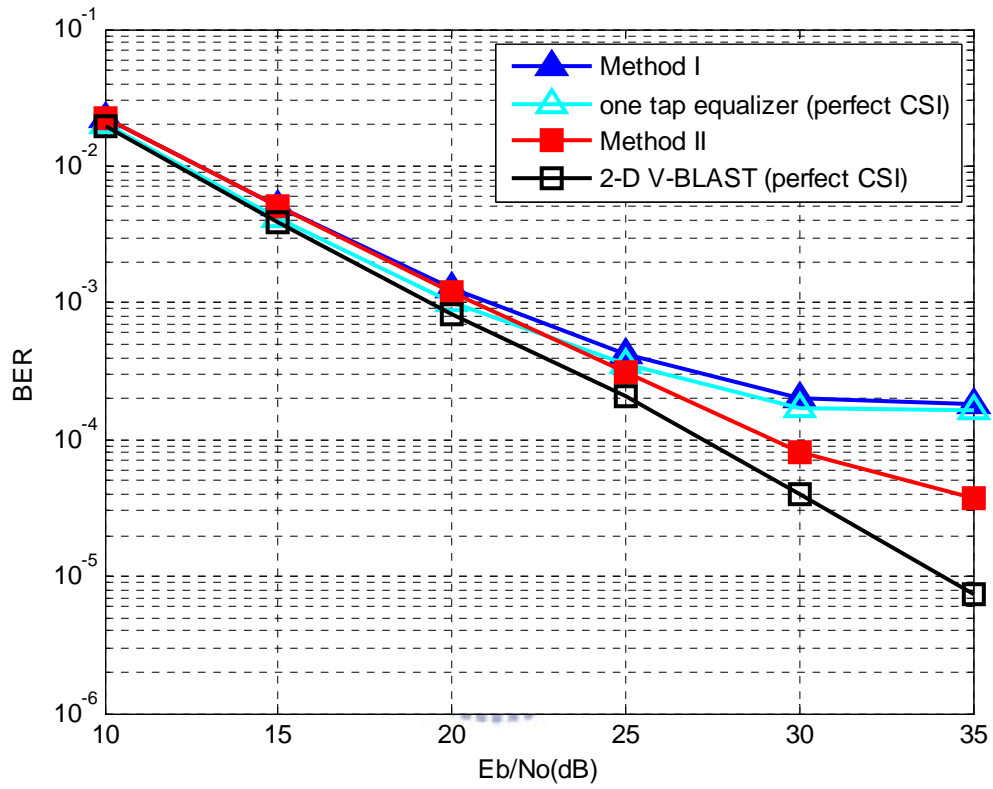


Fig. 9 BER performance in the ITU Veh-B channel for normalized Doppler frequency

$$F_d * T = 0.02$$

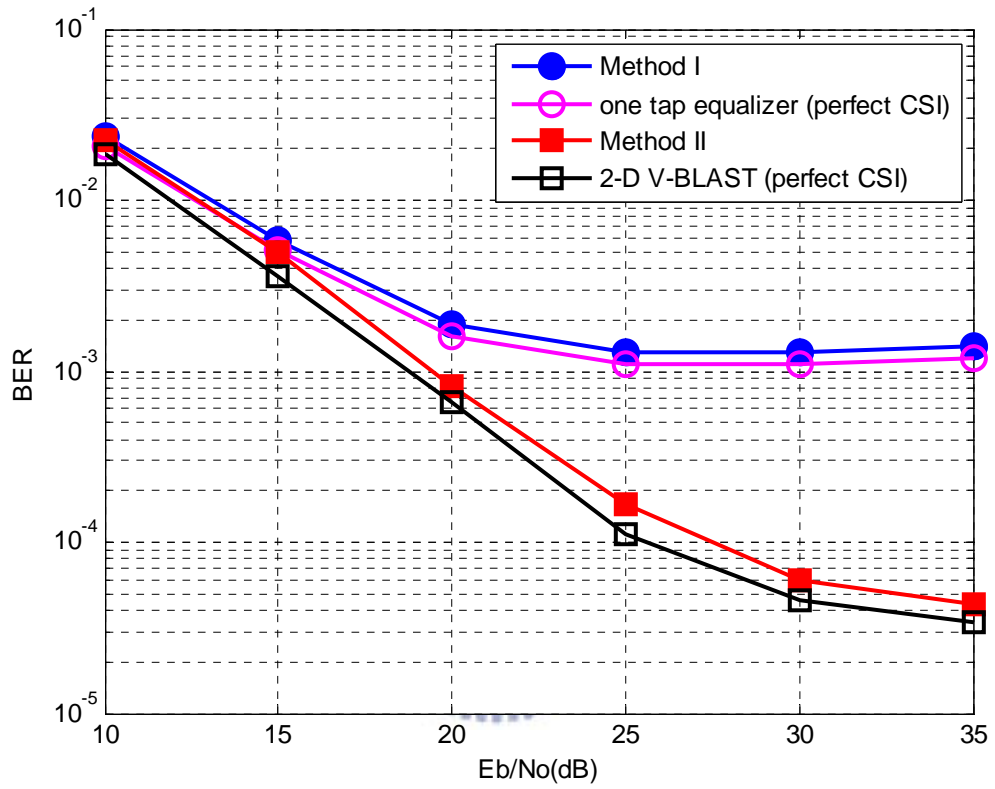


Fig. 10 BER performance in the two-path channel for normalized Doppler frequency

$$F_d * T = 0.05$$

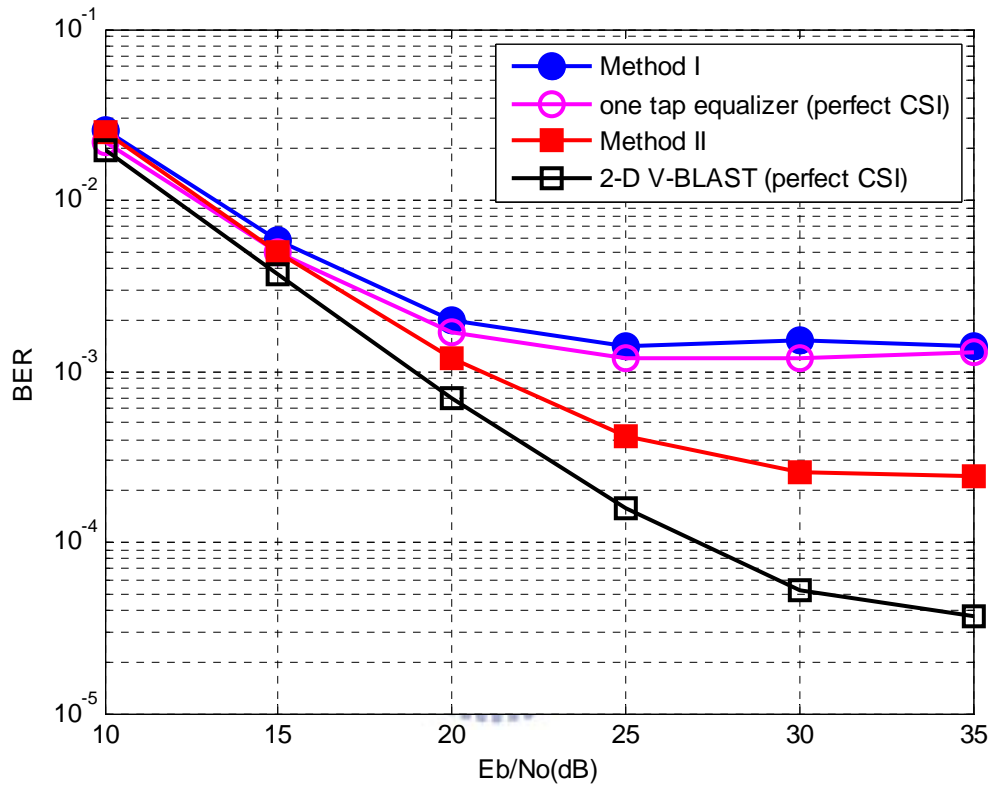


Fig. 11 BER performance in the ITU Veh-B channel for normalized Doppler frequency

$$F_d * T = 0.05$$

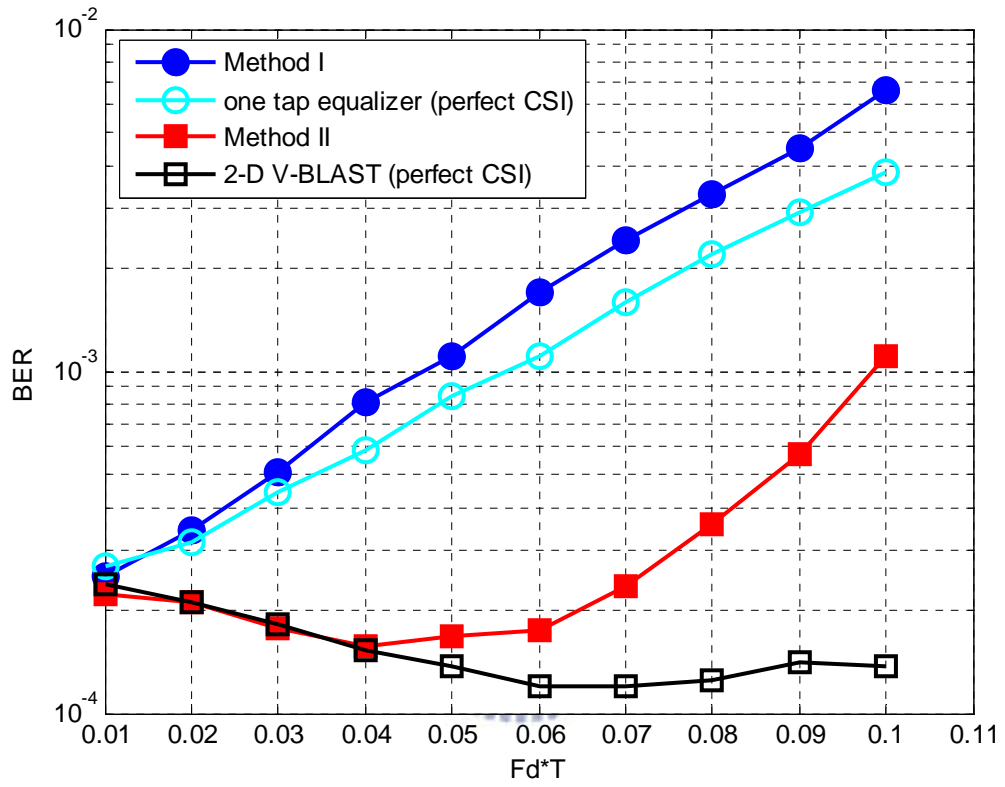


Fig. 12 BER versus normalized Doppler frequency $F_d * T$ in the two-path channel at $E_b / N_o = 25\text{dB}$

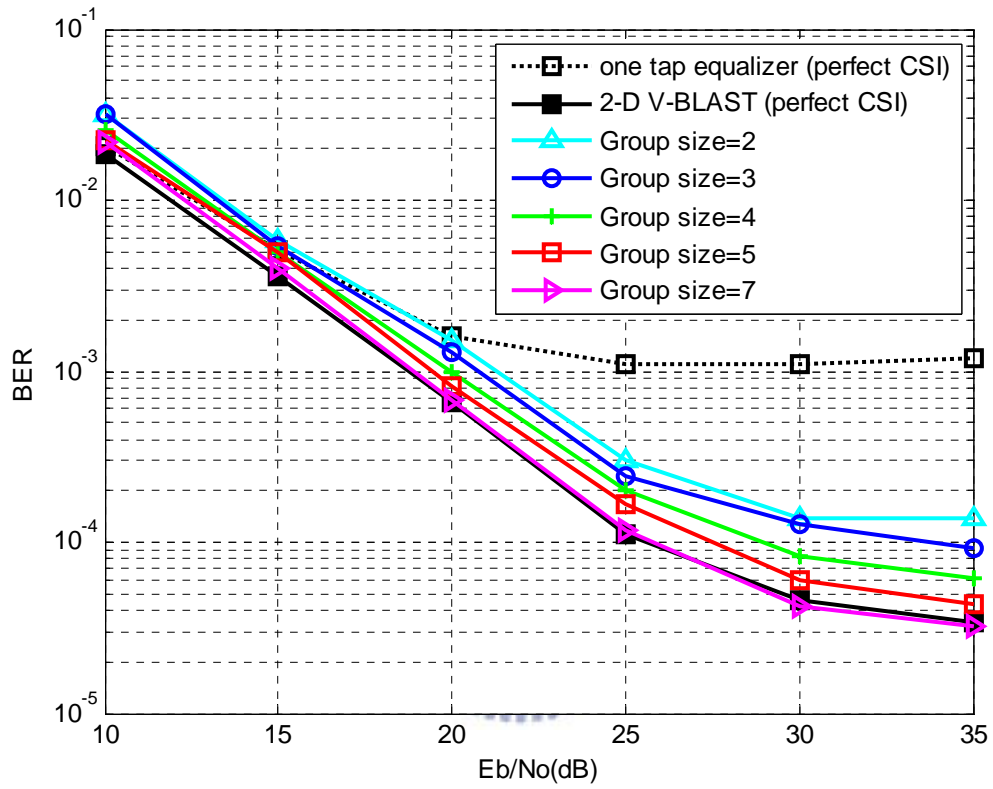


Fig. 13 BER performance in the two-path channel for normalized Doppler frequency

$F_d * T = 0.05$ with different group size.

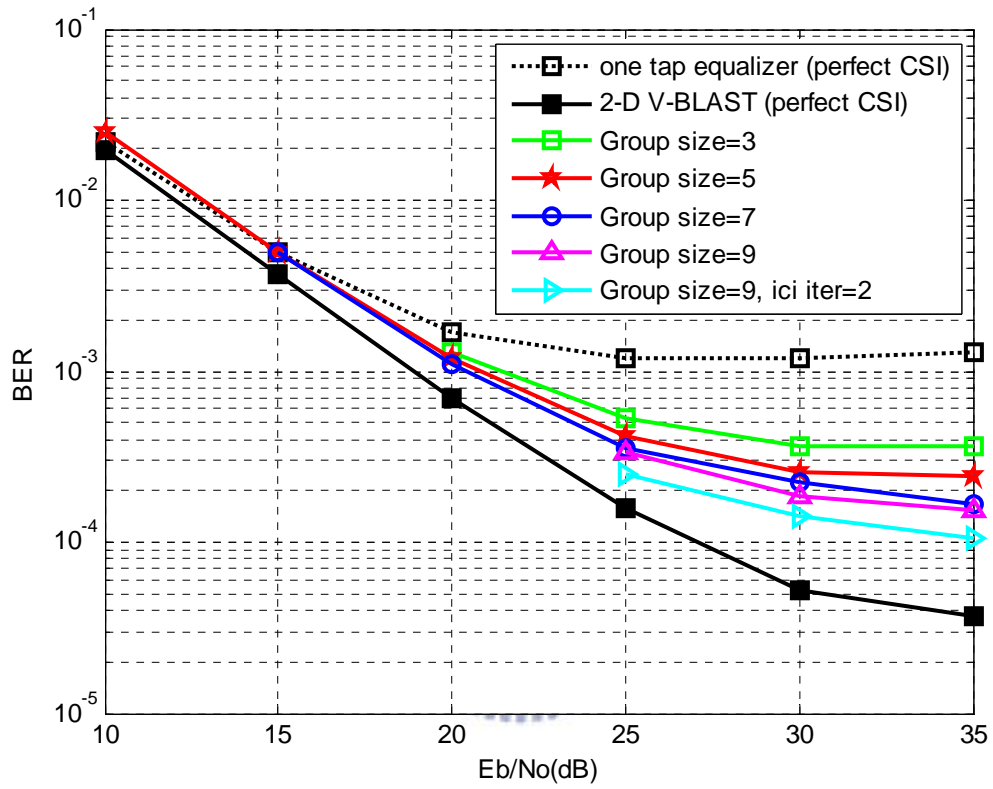


Fig. 14 BER performance in the ITU Veh-B channel for normalized Doppler frequency

$F_d * T = 0.05$ with different group size.

Chapter 6 Conclusions

In this paper, we present an iterative receiver architecture based on joint channel estimation and data detection for MIMO OFDM systems in mobile wireless channels. It mainly consists of three-stage processing. In the initialization stage, an MPIC-based decorrelation method is used to roughly estimate multipath delays and multipath complex gains. In the tracking stage, a β -tracker, followed by decision-feedback (DF) DFT-based channel estimation which is based on V-BLAST data detection is proposed, we can estimate the average channel variations of each path. In the final stage, we adopt a linear model to approximate time variations of each path, and a two-dimensional V-BLAST method is utilized to perform ICI cancellation and data detection. The simulation results show that the β -tracker, followed by decision-feedback (DF) DFT-based channel estimation performs well in high mobility channels, and its BER performance can even approach the case with ideal CSI assumption. Furthermore, the ICI estimation and cancellation can effectively alleviate the error floor and thus significantly improve the performance.

Bibliography

- [1] L. J. Cimini Jr., "Analysis and simulation of a digital mobile channel using orthogonal frequency division multiplexing," *IEEE Trans. Communications*, vol. COM-33, pp.665-675, July 1985.
- [2] P. W. Wolniansky, G. J. Foschini, G. D. Golden, R.A. Valenzuela, "V-BLAST: An Architecture for Realizing Very High Data Rates Over the Rich-Scattering Wireless Channel", in *Proc. Int. Symp. Signals, Systems, and Electronics (ISSSE'98)*, Pisa, Italy, Oct. 1998, pp. 295–300.
- [3] Y. G. Li and L.J. Cimini, "Bounds on the interchannel interference of OFDM in time-varying impairments," *IEEE Transactions on Communications*, vol. 49, pp. 401-404, Mar. 2001.
- [4] Tiejun Wang, John G. Proakis, Elias Masry, and James R. Zeidler, "Performance degradation of OFDM systems due to Doppler spreading," *IEEE Transactions on Wireless Communications*, vol. 5, No. 6, pp. 1422-1432, Jun. 2006.
- [5] A. Seyedi and G. J. Saulnier, "General ICI Self-cancellation Scheme for OFDM Systems," *IEEE Transactions on Vehicular Technology*, vol. 54, no.1, pp. 198-210, Jun. 2006.
- [6] Y. S. Choi, P. J. Voltz, and F. A. Cassara, "On Channel Estimation and Detection for Multicarrier Signals in Fast and Selective Rayleigh Fading Channels," *IEEE Transactions on Communications*, vol. 49, pp. 1375-1387, Aug. 2001.
- [7] Y. Mostofi and D. C. Cox, "ICI Mitigation for Pilot-Aided OFDM Mobile Systems", *IEEE Trans. Commun.*, vol. 4, No. 2, pp. 765-774, Mar. 2005.
- [8] Branka Vucetic, Jinhong Yuan, *Space-Time Coding*, Wiley, Great Britain, 2003.
- [9] Jung-Hyun Park, Mi-Kyung Oh, and Dong-Jo Park, "New channel estimation exploiting reliable decision-feedback symbols for OFDM systems," in *Proc. Int. Conf. on Communicaitons*, pp. 3046-6051, June 2006.
- [10] L. Deneire, P. Vandenameele, L. Van der Perre, B. Gyselinckx, and M. Engels, "A low-complexity ML channel estimator for OFDM," *IEEE Trans. Commun.*, vol.51, no. 2, pp. 135-140, Feb. 2003.
- [11] O. Edfors, M. Sandell, J. J. van de Beek, S. K. Wilson and P. O. Börjesson, "Analysis of

DFT-Based Channel Estimators for OFDM”, in Personal Wireless Commun. Vol. 12, Jan. 2000.

- [12] Meng-Lin Ku and Chia-Chi Huang, “A Derivation on the Equivalence between Newton’s Method and DF DFT-Based Method for Channel Estimation in OFDM Systems”, submitted to IEEE Trans. Wireless Commun..
- [13] Xiaodong Cai and Georgios B. Giannakis, “Bounding Performance and Suppressing Intercarrier Interference in Wireless Mobile OFDM,” IEEE Transactions on Communications, vol. 51, no. 12, pp. 2047-2056, Dec. 2003.
- [14] IEEE Std. 802.16. IEEE Standard for Local and Metropolitan Area Networks Part 16: Air Interface for Fixed Broadband Wireless Access Systems, 2004.
- [15] J. Laiho, A. Wacker, and T. Novosad, Radio Network Planning and Optimization for UMTS. New York: Wiley, 2002.
- [16] W. C. Jakes, Microwave Mobile Communications. New York: Wiley, 1974.

